FINITE ELEMENT METHOD ANALYSIS

OF WIDE-FLANGE BEAM WITH REINFORCED OPENING

by

Farn-Shinn Liou

Diploma, Taipei Institute of Technology, 1964

———————————

A MASTER'S REPORT
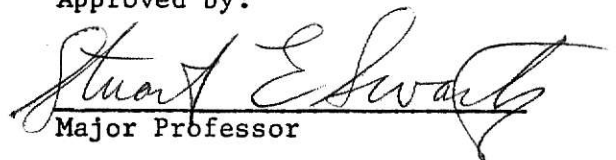
submitted in partial fulfillment of the

requirements for the degree

MASTER OF SCIENCE

Department of Civil Engineering

KANSAS STATE UNIVERSITY

Manhattan, Kansas

1972

Approved by:

Major Professor

Table of Contents

Table of Figures

I. INTRODUCTION

In many buildings, openings through the webs of steel beams are required either for access or for utility installations. Therefore, to find an economic and convenient method for cutting openings and fabricating appropriate reinforcement is necessary. Before 1960, there were more than 70 publications[1,2*] which, either in Russia, or the United States, or other countries, reported on stress concentrations for small round holes through plate and beam webs. In the past few years, researchers have been endeavoring to investigate larger rectangular openings through beam webs. Both analytical and experimental investigations have been made of various openings with and without reinforcing. These investigations were concerned with the stress concentration factor, the necessity for reinforcing, the amount of reinforcing, the location of reinforcing, and the effect of different moment-shear (M/V) ratios for various types of reinforcement.

An investigation has been carried out at Kansas State University[3] including 16 elastic tests, 3 plastic tests and theoretical analyses by using the Vierendeel truss concept for a 6"x9" rectangular web opening at the middepth of a W12x45 steel beam subjected to 4 different loadings with various M/V ratios.

The purpose of this report was; (1) to find an analytical solution by evaluating a reasonable element mechanism to simulate the beam behavior

---

*Superscripts refer to items listed in the References.

with web opening using the finite element method with the ICES-STRUDL computer program, (2) to compare the effects of different lengths of reinforcing bar (see Fig. 1) for a wide-flange beam with web opening, and (3) to obtain a comparison with experimental results and analytical results based on Vierendeel assumptions presented in reference 3.
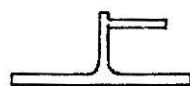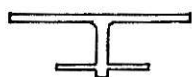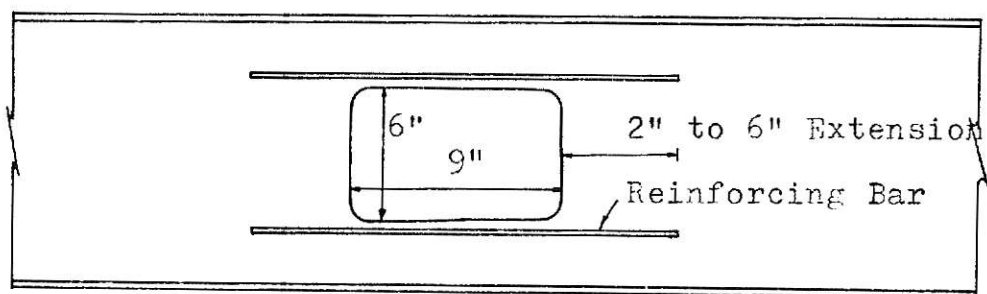
Two-sided Reinforcing   One-sided Reinforcing

Fig. 1 Web Opening and Reinforcing Details

II. LITERATURE REVIEW

In 1932, Muskhelishvili[4] introduced a practical method to solve
plane elasticity problems, particularly for the stress distribution in
a plane weakened by an opening. In 1950, Joseph and Brock[5] used his
complex variable method to obtain an exact solution for the stress con-
centrations around small openings of several shapes subjected to pure
bending.

Using the same method, Heller, Brock and Bart[6], in 1962, presented
a solution for the stress around a rectangular opening with rounded
corners in a uniformly loaded plate. In 1962, they adopted the same
procedures obtaining stress distributions due to bending with shear.[7]
In both cases, they presented curves showing tangential stresses around
the boundary of a typical family of rectangles and the maximum values of
the boundary stress as a function of both aspect ratio and corner ratios.
From curves, they concluded that a basic reduction in stress concentration
occurs with increased radius, and the interaction between stress concen-
trations is equivalent to a mutual cancellation or stress relief.

In 1962, Segner[5] had an investigation concerning the necessity, con-
figuration, amount, and location of openings through a beam web. His
method is based on the concept that a member with such an opening
has points of contraflexure centered above and below the opening at the
center line. He then verified this by laboratory data. He gave the con-
clusion that, on the basis of test results and cost comparisons, the most
satisfactory configuration for reinforcement is as shown in Fig. 2. The

yield load moment of the reinforced section is only about 70% of that for the original gross section, but there is no significant difference in the ultimate moment between them. He recommended that reducing the ratio of opening depth to girder depth, or relocating the opening within the span would be the approach to save cost.
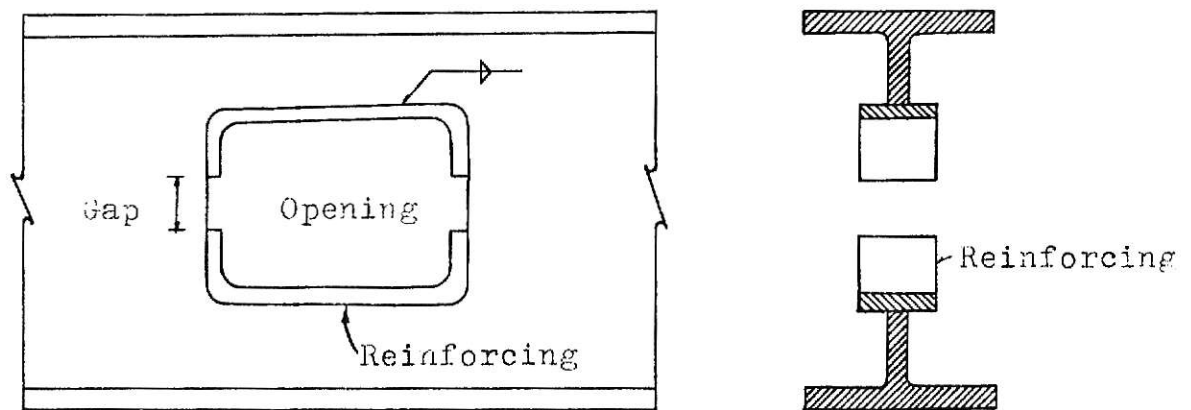
Fig. 2 The Ideal Reinforcement

In 1962, Snell[8] used the finite element method to analyze a rectangular plate with opening of one-third the width of the plate subjected to uniaxial tension in a plane stress field. He found that the maximum stress concentration is 3.65. The finite element method, with element size of one-twelfth of the opening in linear length, gave an average stress concentration in the critical element as 3.31. He also suggested two approaches to reduce the stress concentration occuring around the opening in a plate. The first method involved adding reinforcing at the points of high stress, while the second method adds reinforcing in such a way that

it draws the stress away from the opening. He found that ring reinforcement resulted in a decrease of 30% in the stress concentration, while using strip type reinforcing with the same amount of reinforcing in a favorable location gave 23% reduction. In the same case, for strip type reinforcing with double the amount of reinforcing, the reduction in stress concentration was 36%. The test series indicated that the most effective length for strip reinforcing was closely approximated by placing the reinforcing in such a way that the ends of reinforcing are on lines drawn outward from the corners of the opening in the plate at a 45° angle to the plate axes.

In 1966, an analytical method for calculating stresses around elliptical holes in a wide-flange beam under a uniform load was presented by Bower[9]. The applicability of the analysis depends on the hole size and on the magnitude of the M/V ratio at the hole. For circular holes, boundary conditions at the hole for moment equality are satisfied when the ratio of beam depth to hole diameter is 2.0 or greater. The results also indicated that for a M-V ratio of 4.8/L, in which L is the span length of the beam, a depth ratio of 6.0 is required to satisfy shear-moment equality. In the same year, he conducted tests on simply supported wide-flange beams with and without cantilever action having circular or rectangular web openings loaded by concentrated loads.[10] He concluded that the elastic analysis can accurately predict the tangential stress along the hole and the bending stress on transverse cross sections in the vicinity of the hole for circular and rectangular openings not exceeding half of the web depth. He also concluded that the Vierendeel method predicts a reasonably accurate bending

stress except for local stress concentrations at the opening corners.

In 1968, Redwood and McCutheon[11] reported some tests to failure of steel wide-flange beams containing one or two unreinforced openings. The openings are various shapes but all have the same height which is equal to 57% of the beam depth. The experimental results indicated that under pure bending the moment capacity of the beams with one or two openings can be calculated based on the plastic modulus of the net section through the opening. The presence of shear reduces the moment capacity of the beam at the opening below that for pure bending. The reduction is a function of opening shape, dimensions, the spacing of openings, and the shear/moment ratio. The presence of an adjacent circular opening at the spacings tested did not reduce the strength below that of a beam containing a single circular opening. At the M-V ratio of 0.425, the moment capacity reduces to 64% - 72% for both simple and double circular openings, and reduces to 40% for a single rectangular opening.

In 1968, Bower[12] suggested the criteria for elastic design, plastic design, and buckling design. He concluded that, for elastic design, beams with web holes should be designed using the same basic factors of safety against yielding as in the AISC specification, except that the maximum allowable bending and shear stresses should be computed using the actual stresses causing yielding at the hole rather than nominal beam stresses. For plastic design, beams with web holes should be designed using the AISC load factor of 1.70, except that the maximum allowable loads should be computed using the actual ultimate strength of the beam at the hole rather than the strength of the gross beam. For large spacings

of holes, the effects of each hole should be computed individually. For more than two adjacent holes, use Vierendeel frame analysis; for geometrically dissimilar adjacent holes, use a frame analysis. With regard to buckling, beams with holes are subject to the same types of buckling as beams without holes. However, some possible buckling modes may be more likely to occur in beams with holes than in beams without holes. The AISC formula for web crippling is applicable for beams with holes, so long as the edge of the hole is at least 4" from the edge of bearing. When a hole is located in a region of pure bending, the possibility of vertical flange buckling could be checked by assuming that the compression T-section at the hole acts as a column.

In 1969, Cheng conducted a test of a rectangular opening with round corners in a wide-flange beam subjected to combined bending and shear using the photostress method in conjunction with electrical resistance strain gages.[13] He concluded that larger deflections are to be expected in a beam with web openings and can be well predicted by elastic theory. Simple beam theory can not be used to predict the normal stress which is non-linear in a region extending from the edge of the opening a distance about equal to the depth of the beam from the opening.

In 1970, Congdon and Redwood[14] conducted an investigation concerning the plastic analysis of reinforced openings through beam webs based on the assumption of perfectly plastic material behavior. A series of tests were carried out to determine the effects of M-V ratio, reinforced area, hole aspect ratio, ratio of hole depth to beam depth, and location of

reinforcement on the beam behavior. The experimental results confirmed the assumption of simple stress distribution at failure. The equation for figuring out the area of reinforcement to take maximum shear capacity was also provided. The effects due to one-sided reinforcement for the web opening are not much different from those obtained from reinforcement on both sides of the web at critical points.

III. METHOD OF ANALYSIS

A. Introduction

Knowledge of the force-displacement relationships and material properties is necessary in order to solve structural engineering problems. The classical techniques of structural analysis used to solve these problems use either the displacement compatibility approach or the force equilibrium approach. In the conventional structural analysis the member dimensions and the explicit stress-strain relationships are generally known. Analyses of complex structures, composed of beams, plates, grids, etc., are too complicated to be handled either by the beam theory or the classical continuum mechanics approaches. With the help of the digital computer, matrix operation methods meet the needs for the analysis of complex structures.

The direct stiffness method is generally preferred over the force method and other displacement methods. Its apparent advantages are, (1), no need for having to select the redundant forces before the structural stiffness matrix is formulated; (2), the structural stiffness matrix is usually sparsely populated and banded along the principal diagonal; (3), no excessive operation of triple matrix multiplication is needed to form the structural stiffness matrix.

The initial development of the direct stiffness method was by Levy[15] who introduced the idea of replacing the continuous structure by parts or elements, finding a stiffness matrix for each element, and then combining these stiffness matrices. Turner et al.[15] refined this application by assuming the real continuum to be divided into assemblies of imaginary,

finite triangular, or rectangular slices interconnected only at a finite number of nodal points on their boundaries at which some equivalent forces, representative of the distributed stresses actually acting on the element boundaries, were supposed to be considered. The displacements of these nodal points are the basic unknown parameters of the whole problem. The state of displacement within each finite element is defined uniquely by a displacement function in terms of its nodal displacements. Therefore the state of strain, and the state of stress are also defined by this function throughout the element including its boundaries. Once these stages have been reached, we can find the element stiffness matrix by the energy method and follow the standard direct stiffness method.

The new idea of the finite element method is the analysis of the stiffness characteristics of arbitrary two or three dimensional elements. Using such elements, the structural idealization is obtained by dividing the original continuum into segments of appropriate sizes and shapes, all of the material properties of the original system being retained in the individual elements.

B. The Direct Stiffness Method

(a). Derivation of element force-displacement equation

For each element, relationships between forces (equivalent to the distributed forces on the element boundaries) and displacements at the node points can be derived in matrix form referred to the local coordinates:

$$\{f\} = [\bar{k}]\, \{\delta\}$$

where $\{f\}$ and $\{\delta\}$ are column matrices of forces and displacements respectively at the nodes, and $[\bar{k}]$ is a square, element stiffness matrix referred to the local coordinate axes.

(b). Transformation of the element stiffness matrix

Each element stiffness matrix must then be transformed from the local coordinate system to the global coordinate system of the complete structure.[16]

$$[k] = [T]^T [\bar{k}]\, [T] \tag{2}$$

where $[k]$ is the element stiffness matrix referred to the global coordinates, $[T]$ is the transformation matrix relating the local coordinates and the global coordinates, and $[T]^T$ is the transpose of $[T]$.

(c). Assembly of the total stiffness matrix

The element stiffness matrix can be expressed as

$$[k^1] = \begin{pmatrix} k_{ii}^1 & k_{ij}^1 \\ k_{ji}^1 & k_{jj}^1 \end{pmatrix} \tag{3}$$

for each element. The superscripts refer to the element number and the subscripts are refered to the joint name as shown on Fig. 3. For the entire structure, the total stiffness matrix is obtained by superposition of each of the element stiffness matrices.

$$[K] = \begin{pmatrix} k_{ii}^1 & k_{jj}^1 & & o & o & o \\ k_{ji}^1 & k_{jj}^1 + k_{jj}^2 + k_{jj}^3 + k_{jj}^4 & k_{jk}^2 & k_{jl}^3 & k_{jm}^4 \\ o & k_{kj}^2 & k_{kk}^2 & o & o \\ o & k_{lj}^3 & o & k_{ll}^3 & o \\ o & k_{mj}^4 & o & o & k_{mm}^4 \end{pmatrix} \tag{4}$$

It is easy to visualize that member 2 connecting joints j and k will only influence the equilibrium equations of these two joints, and therefore will only affect the elements k_{jj}, k_{jk}, k_{kj}, and k_{kk} of the complete structure stiffness matrix.

The force-displacement relation for the entire structure is then

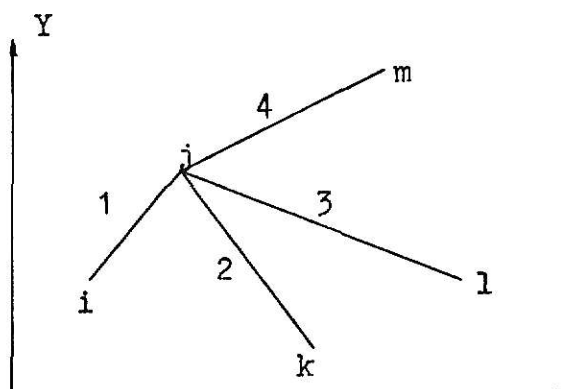$$\{F\} = [K] \{U\} + \{F_0\} \tag{5}$$

Fig. 3   Element Assembly

where $\{F\}$ is the column matrix of applied external loads including re-
actions, $\{F_0\}$ is the column matrix of nodal forces introduced to maintain
the initial structural shape in the presence of thermal gradients or
equivalent effects, $[K]$ is the total stiffness matrix, and $\{U\}$ is the
column matrix of actual nodal displacements of whole structure.

(d).   Determination of nodal displacements

The complete structural stiffness matrix $[K]$ is singular and can-
not be inverted. However, the set of Eqs. (5) can be arranged and
partitioned so that

$$\left\{- \frac{F'}{R} -\right\} = \left[- \frac{K_{11}}{K_{21}} - \left|\vphantom{\frac{}{}}\right. - \frac{K_{12}}{K_{22}} -\right] \left\{- \frac{U'}{C} -\right\} \tag{6}$$

where $\{F'\}$ are the specified loads applied to the structure, $\{R\}$ are the
reactions at points of support or constrained deflections, $\{U'\}$ are the
unknown displacements, and $\{C\}$ are the specified displacements (zero for

undeformed support points). For the case of the presence of thermal gradients, the column matrix on left side of Eqs. (5) includes Fo, i.e., $F = F-Fo$. The unknown displacements may then be found as

$$\{U'\} = [K_{11}]^{-1} \left[\{F'\} - [K_{12}] \{C\} \right] \tag{7}$$

The reactions can be obtained in terms of the nodal displacements as,

$$\{R\} = [K_{21}] \{U'\} + [K_{22}] \{C\} \tag{8}$$

(e). Determination of stresses

In each element, stresses (or internal loads) may be found directly from the nodal displacements:[16]

$$\{\sigma\} = [s] \{\delta\} \tag{9}$$

where [s] is the stress matrix for the elements.

(f). Comments on the complete structural stiffness matrix[16]

(1). The set up of the structural stiffness matrix does not need to refer to loading or boundary conditions or to redundancy.

(2). All terms along the main diagonal of the structural stiffness matrix are positive, which means that the directions of forces and corresponding displacements are coincident.

(3). The sum of the elements in any column of the complete structural stiffness matrix is zero, which reflects adherence to the conditions of equilibrium.

(4). It is seen that the total stiffness matrix is always symmetric

and is always singular. The symmetric property reveals the truth of Maxwell's reciprocal theorem. The singularity of the stiffness matrix represents the possible rigid-body motion of the structure.

(5). Stability of the structural element arrangement is assured if the inversion process in determining the unknown displacements can be carried out. In other words, on specifying adequate conditions on the displacements, sufficient to prevent rigid-body motion, the singularity present in the structural matrix will be removed. For instance, the reduced stiffness matrix $[K_{11}]$ is nonsingular for a statically stable structure and can be inverted.

(6). Alternative boundary conditions can be studied by merely rearranging the partitioning of the structural stiffness matrix and proceeding with the solution as before.

(7). Members may be removed, or new ones added, by simply introducing the necessary changes into the appropriate local elements of the complete structural stiffness matrix.

C. Formulation of the Finite Element Method

(a). Introduction

Certain approximations have been introduced into the formulation of the finite element in the discretization of the original continuum and the evaluation of element properties. Judgement is required in making the proper subdivision, such as element shape and degrees of freedom, so that the substitute structure can simulate the actual structure. It is also important to choose a suitable displacement function which can satisfy the requirement of displacement continuity between adjoint elements. All of these factors will determine whether the substitute structure is stiffer or more flexible than the real structure and to what degree the approximation is acceptable.

In brief, the finite element technique has the following character-istics:

(1). Structural discretization;

(2). Necessity for choosing proper displacement functions;

(3). Evaluation of element properties;

(4). Assemblage of finite elements and following the standard displacement method procedures.

In applying this method, the following requirements must be satisfied simultaneously:

(1). Force equilibrium in each element;

(2). Displacement compatibility at nodal points between adjacent elements;

(3). The internal forces and deformations are related through the geometric and material property characteristics.

(b). Plane stress in plate —— triangular element

The first civil engineering applications of the finite element technique have been in studies of plane stress and plane strain.

Various shapes of finite elements were employed in these analyses. In general, applicable rectangular elements give a little better approximation of stresses and deflections for a given nodal pattern than triangular elements, because they employ a closer deformation approximation. However the use of quadrilateral elements could entail arithmetical difficulty and consequently a disproportionate increase of computing time in deriving the element characteristics. Because of greater adaptability of the triangular shape in fitting arbitrary boundary geometries, triangular elements will be used here.

(1) Displacement functions

Consider an arbitrary triangular element with nodes i, j, m numbered in an anti-clockwise order as shown in Fig. 4. The plane displacements of a node have two components

$$\{\delta_i\} = \begin{Bmatrix} u_i \\ v_i \end{Bmatrix} \tag{10}$$

THIS BOOK CONTAINS NUMEROUS PAGES WITH DIAGRAMS THAT ARE CROOKED COMPAIRED TO THE REST OF THE INFORMATION ON THE PAGE.
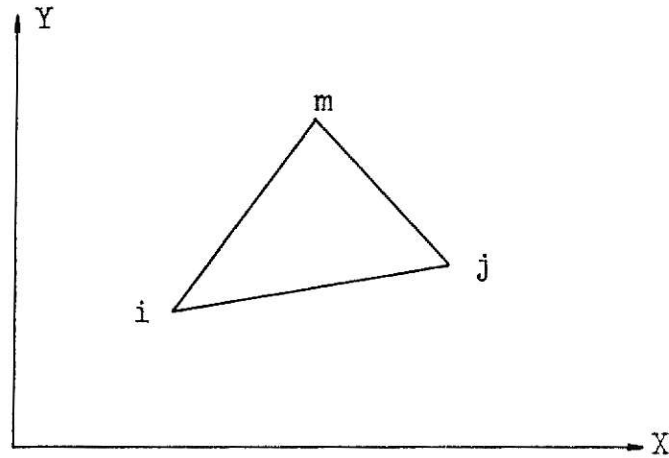
THIS IS AS RECEIVED FROM CUSTOMER.

Fig. 4 Element Incidences

and the six components of element displacement can be listed as a column matrix

$$\{\delta\} = \begin{Bmatrix} \delta_i \\ \delta_j \\ \delta_m \end{Bmatrix} \tag{11}$$

Assume the following parametric displacement field for the two displacement components at any point within each element:

$$u^e = \alpha_1 + \alpha_2 x + \alpha_3 y$$

$$v^e = \alpha_4 + \alpha_5 x + \alpha_6 y \tag{12}$$

These two equations can be expressed in the general form as

$$\begin{Bmatrix} u\ (x,y) \\ v\ (x,y) \end{Bmatrix}^e = [N]\{\alpha\}^e = \begin{pmatrix} 1 & x & y & o & o & o \\ o & o & o & 1 & x & y \end{pmatrix} \begin{Bmatrix} \alpha_1 \\ \alpha_2 \\ \alpha_3 \\ \alpha_4 \\ \alpha_5 \\ \alpha_6 \end{Bmatrix} \tag{13}$$

where $[N]$ and $\{\alpha\}^e$ are displacement functions and undetermined coefficients respectively. Evaluate nodal displacement components in terms of the undetermined coefficients:

$$\{\delta\} = [A]\ \{\alpha\} \tag{14}$$

On substituting the boundary conditions in Eq. 13,

$$u_i = \alpha_1 + \alpha_2 x_i + \alpha_3 y_i,$$

$$u_j = \alpha_1 + \alpha_2 x_j + \alpha_3 y_j,$$

$$u_m = \alpha_1 + \alpha_2 x_m + \alpha_3 y_m,$$

$$V_i = \alpha_4 + \alpha_5 x_i + \alpha_6 y_i, \tag{15}$$

$$V_j = \alpha_4 + \alpha_5 x_j + \alpha_6 y_j,$$

$$V_m = \alpha_4 + \alpha_5 x_m + \alpha_6 y_m\ .$$

These equations reveal the square matrix $[A]$ as

$$[A] = \begin{pmatrix} 1 & x_i & y_i & o & o & o \\ 1 & x_j & y_j & o & o & o \\ 1 & x_m & y_m & o & o & o \\ o & o & o & 1 & x_i & y_i \\ o & o & o & 1 & x_j & y_j \\ o & o & o & 1 & x_m & y_m \end{pmatrix} = \begin{pmatrix} A_{11} & \vdots & o \\ \cdots & \vdots & \cdots \\ o & \vdots & A_{11} \end{pmatrix} \tag{16}$$

This will be square if the number of displacement functions has been taken

equal to the number of nodal displacement components. Solving these equations by sub-matrix for α_1, α_2, α_3, α_4, α_5, and α_6 in terms of the nodal displacements u_i, u_j, u_m, V_i, V_j, and V_m, i.e.,

$$\{\alpha\} = [A^{-1}]\{\delta\} \tag{17}$$

and substituting into Eqs. (13), we can obtain finally

$$u = \frac{1}{2\Delta} [(a_i + b_i x + c_i y) u_i + (a_j + b_j x + c_j y) u_j + (a_m + b_m x + c_m y)u_m] \quad \text{and} \tag{18}$$

$$v = \frac{1}{2\Delta} [(a_i + b_i x + c_i y) v_i + (a_j + b_j x + c_j y) v_j + (a_m + b_m x + c_m y) v_m]$$

in which

$$a_i = x_j y_m - x_m y_j \quad ,$$

$$b_i = y_j - y_m = y_{jm} \quad ,$$

$$c_i = x_m - x_j = x_{mj} \quad ,$$

$$a_j = x_m y_i - x_i y_m \quad ,$$

$$b_j = y_m - y_i = y_{mi} \quad ,$$

$$c_j = x_i - x_m = x_{im} \quad ,$$

$$a_m = x_i y_j - x_j y_i \quad ,$$

$$b_m = y_i - y_j = y_{ij} \quad ,$$

$$c_m = x_j - x_i \, x_{ji} \quad .$$

Also

$$2\Delta = \det \begin{vmatrix} 1 & x_i & y_i \\ 1 & x_j & y_j \\ 1 & x_m & y_m \end{vmatrix} = 2 \text{ (area of triangle i, j, m)} \tag{19}$$

Eqs. (18) can be represented in the form of eqs. (13):

$$\begin{Bmatrix} u(x,y) \\ v(x,y) \end{Bmatrix}^e = [N] \{\delta\} = [IN_i', \ IN_j', \ IN_m'] \{\delta\} \tag{13A}$$

with I a two by two identity matrix, and

$$N_i' = \frac{a_i + b_i x + c_i y}{2\Delta} \quad ,$$

$$N_j' = \frac{a_j + b_j x + c_j y}{2\Delta} \tag{20}$$

$$N_m' = \frac{a_m + b_m x + c_m y}{2\Delta}$$

If the coordinates are taken from the centroid of the element for the simplification of the calculation then

$$x_i + x_j + x_m = y_i + y_j + y_m = o \text{ and}$$

$$a_i = \frac{2\Delta}{3} = a_j = a_m \tag{21}$$

From Eqs. (18) we find that the displacement varies linearly along any side of the triangular element and has identical values at the nodes. This therefore guarantees the continuity of displacements with adjacent elements.

(2). Strain

In the determination of the strain-displacement relationship for the element, it is assumed that small deflection theory of classical elasticity is applicable. The internal strains can be obtained as follows:

$$\{\varepsilon\} = \left\{ \begin{array}{c} \varepsilon_x \\ \\ \varepsilon_y \\ \\ \gamma_{xy} \end{array} \right\} = \left\{ \begin{array}{c} \dfrac{\partial u}{\partial x} \\ \\ \dfrac{\partial v}{\partial y} \\ \\ \dfrac{\partial u}{\partial y} + \dfrac{\partial v}{\partial x} \end{array} \right\} \tag{22}$$

Taking the appropriate partial derivatives of Eqs. (18), gives

$$\{\varepsilon\} = \frac{1}{2\Delta} \begin{pmatrix} b_i, & o, & b_j, & o, & b_m, & o \\ o, & c_i, & o, & c_j, & o, & c_m \\ c_i, & b_i, & c_j, & b_j, & c_m, & b_m \end{pmatrix} \{\delta\} = [B] \{\delta\} \tag{23}$$

Obviously, the [B] matrix is independent of the position within the element, and hence the strains are constant throughout. There are some initial strains which are caused by shrinkage, crystal growth, or

temperature change, which are independent of stress and usually are defined by average, constant values. This is consistent with constant strain conditions.

(3). Stress and elasticity matrix

For plane stress in an isotropic material, the stress-strain relationship can be obtained from Hooke's law as

$$\epsilon_x - (\epsilon_x)_o = \frac{\sigma_x}{E} - v\frac{\sigma_y}{E}$$

$$\epsilon_y - (\epsilon_y)_o = -v\frac{\sigma_x}{E} + \frac{\sigma_y}{E} \qquad (24)$$

$$\gamma_{xy} - (\gamma_{xy})_o = 2(1 + v)\frac{\tau_{xy}}{E}$$

where $(\epsilon_x)_o$, $(\epsilon_y)_o$ and $(\gamma_{xy})_o$ are initial strains. Solving for stresses,

$$\begin{Bmatrix} \sigma_x \\ \sigma_y \\ \tau_{xy} \end{Bmatrix} = [D] \begin{Bmatrix} \epsilon_x - \epsilon_{xo} \\ \epsilon_y - \epsilon_{yo} \\ \gamma_{xy} - \gamma_{xyo} \end{Bmatrix} \qquad (25)$$

is obtained, where

$$[D] = \frac{E}{1-v^2} \begin{bmatrix} 1 & v & o \\ v & 1 & o \\ o & o & \frac{(1-v)}{2} \end{bmatrix}, \qquad (26)$$

E = elastic modulus, and

$$v = \text{Poisson's ratio.}$$

For the plane strain case, a similar procedure can be followed to find the [D] matrix.

(4). The stiffness matrix

Let $\{f\}$ be the nodal forces which are equivalent statically to the boundary stresses and distributed loads on the element. By applying virtual displacements of $\{\delta'\}$ at the nodes, the following equation must be satisfied.

$$dW_i = dW_e \qquad (27)$$

Where dW_i is the internal virtual work and dW_e is the external work associate with the virtual displacements.

$$dW_e = \{\delta'\}^T \{f\} \qquad (28)$$

$$dW_i = \int_{vol} \{\varepsilon'\}^T \{\sigma\} \, dV$$

$$= \int_{vol} \{\delta'\}^T [B]^T [D] [B] \{\delta\} \, dV$$

$$= \{\delta'\}^T \left(\int_{vol} [B]^T [D] [B] \, dV \right) \{\delta\} \qquad (29)$$

Where $\{\varepsilon'\}$ is the matrix of the virtual strains induced by virtual displacements $\{\delta'\}$, and $\{\sigma\}$ is the matrix of the actual stresses associated with the nodal forces $\{f\}$.

Introducing unit values of the virtual displacement components in sequence and substituting into equation (27) yields

$$\{f\} = \left(\int_{vol} [B]^T [D] [B] \ dv \right) \{\delta\} \tag{30}$$

By definition, the bracketed term then represents the element stiffness matrix.

The integration indicated in the equation presents no problem for this element since none of the matrices involved is a function of the coordinates x and y. Thus the triple product $[B]^T [D][B]$ is constant and can be taken outside the integral sign. The remaining integral is simply the volume of the element, or $\Delta \cdot t$ when the plate thickness t is constant.

$$[k] = [B]^T [D] [B] \ t\Delta \tag{31}$$

IV. NUMERICAL EXAMPLES

A. Review of Experimental Set Up

The experimental tests in reference 3 were conducted on three W 12 x 45 steel beams which were subjected to a single concentrated load at mid-span and simply supported on the ends. By varying the length of the shear span from 100 in. to 40 in. in increments of 20 in. as shown in Fig. 5, four values of the moment-shear ratio at the opening were studied.

Fig. 1 shows that for each beam the web opening was 6" deep and 9" long with a 1/2" corner radius and centered on the centroidal axis of the beam. Thus, the opening width to depth ratio was 1.5 and the nominal ratio of depth of opening to depth of beam was 0.5.

One series of tests was made without reinforcing and three series of tests were conducted with reinforcing bars.

The type of reinforcing used on the test specimen consisted of rectangular cross section bars oriented parallel to the beam flanges and welded to the web above and below the opening. Four inch extension and six inch extension of the reinforcing bars beyond the edges of the opening were used in separate tests.

With the same cross sectional area of reinforcing bar, either one-sided reinforcing or two-sided reinforcing was tested as shown in Fig. 1.

The cross sectional dimensions of the beam used in the study were the nominal values as indicated in Fig. 6a. The modulus of elasticity was 29,000 ksi, the modulus of rigidity was 11,150 ksi, and the Poisson's ratio was taken as 0.3.
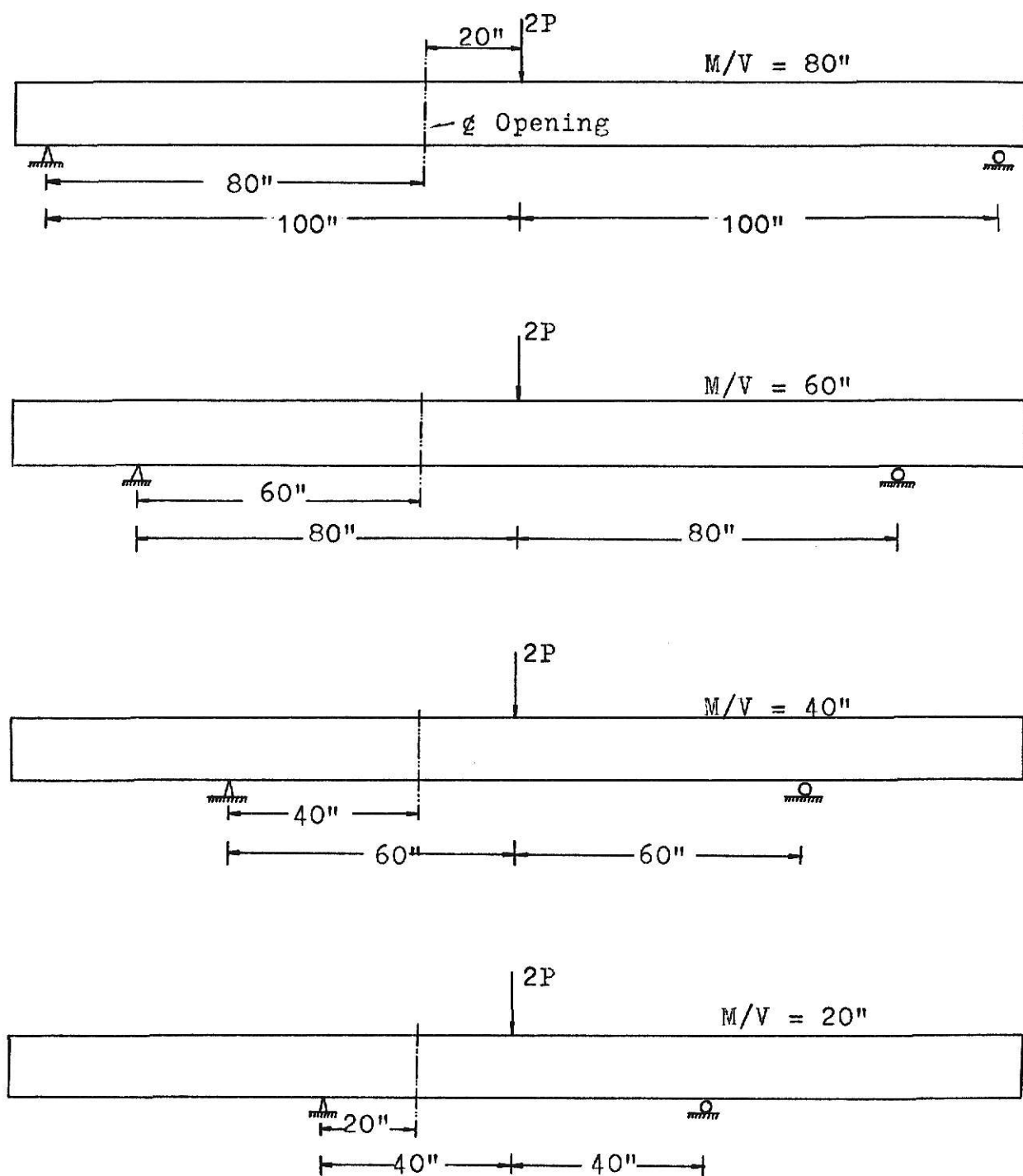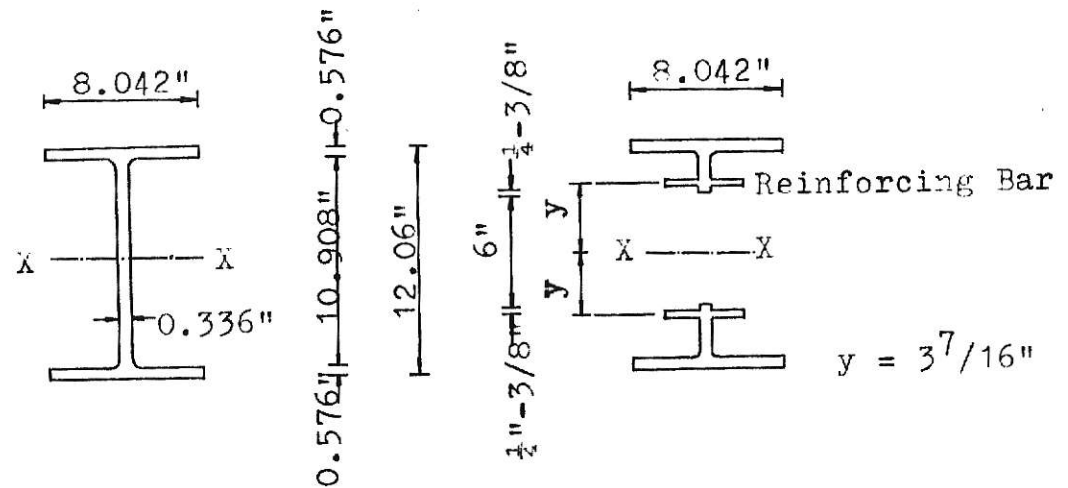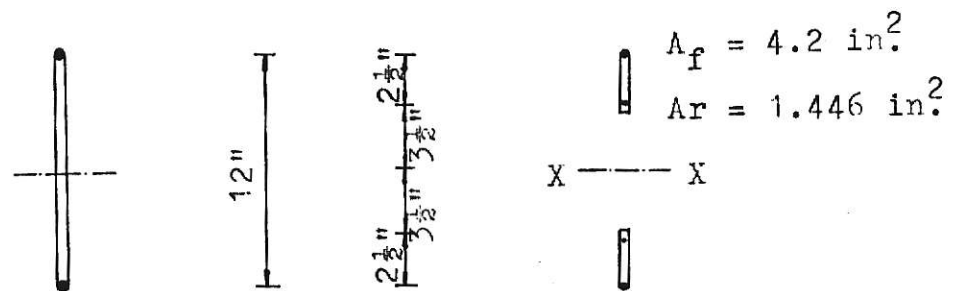
20" 2P

M/V = 80"

¢ Opening

80"

100" 100"

2P

M/V = 60"

60"

80" 80"

2P

M/V = 40"

40"

60" 60"

2P

M/V = 20"

20"

40" 40"

Fig. 5 Experimental Set Up

8.042"

0.576" | 0.576"

10.908"

12.06"

6"

¼ - 3/8"

¼"- 3/8"

0.576"

X ———— X

0.336"

8.042"

Reinforcing Bar

y

y

X ——— X

y = 3⁷/16"

a. Cross Sections of Beam

$A = 13.2 \ in.^2, \quad I_{xx} = 351 \ in.^4$

12"

$2\frac{1}{2}$"

$3\frac{1}{2}$"

$2\frac{1}{2}$"

$3\frac{1}{2}$"

X ——— X

$A_f = 4.2 \ in.^2$

$A_r = 1.446 \ in.^2$

$$I_{xx} = \frac{1}{12} \ b_w \ (h_w)^3 + 2 \ A_f \ y^2$$

$$A^f = (I_{xx} - \frac{1}{12} \ b_w \ h_w^3) \ / \ (2y^2)$$

$$= (351 - 0.336 \cdot 1728/12)/(2 \cdot 6^2) = 4.20 \ in.^2$$

$$A \cdot y^2 = A_r \cdot y_r^2$$

$$A_r = 1.5 \cdot (3.4375)^2 \ / \ (3.5)^2 = 1.446 in.^2$$

b. Idealized Cross Sections of Beam

Fig. 6   Beam Dimensions of Actual & Idealized
Cross Sections

B. Simplification of the Problem

The three dimensional structure was modified to meet the need of the analysis using the plane stress finite element method. The procedure followed was to substitute equivalent bar members pin-connected to the appropriate nodes of the plate elements for the flanges and reinforcing bars. These bar members have one dimensional material properties which can transfer only axial forces.

Since we are more interested in the stress concentration around the opening, only a portion of the beam was studied. It is assumed that the influence of the opening on the stress distribution is no longer significant at a distance of one beam depth from the edge of the opening due to Saint-Venant's principle. A cut portion 30" long centered on the centroidal axes of the opening as shown in Fig. 7 was studied.
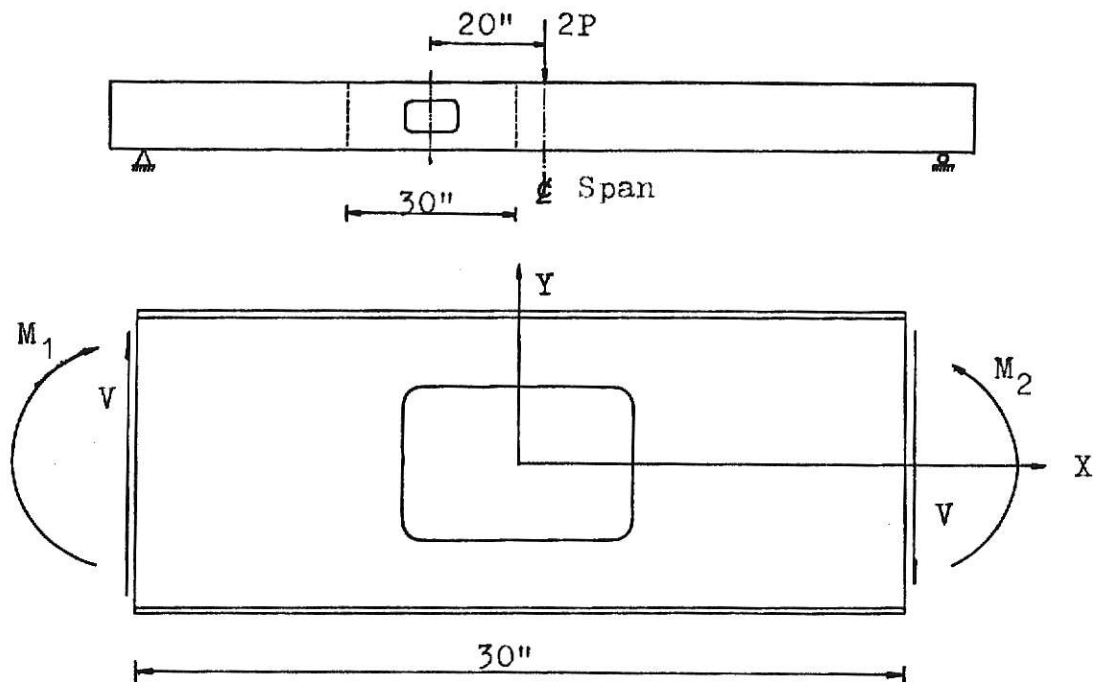
Fig. 7 Portion of Beam Used in Analysis

The idealization, using a plane stress procedure to simulate the beam behavior of one-sided reinforcing, was also included in case that kind of reinforcing was adopted. This is based on the conclusion in references (3, 14) that the one-sided reinforcing makes no discernible effects different from those of the two-sided reinforcing. Therefore, the results of this study can represent both types of reinforcing with the same total cross sectional area.

As shown in Fig. 6b, the shapes of flanges and reinforcing were shrunk to points in order to meet the needs of the plane stress analysis procedure. Also the distances from centroids of flanges and reinforcing to the neutral axis of the beam were readjusted from the original places in the test specimen to be in accord with the arrangement of the discretization.
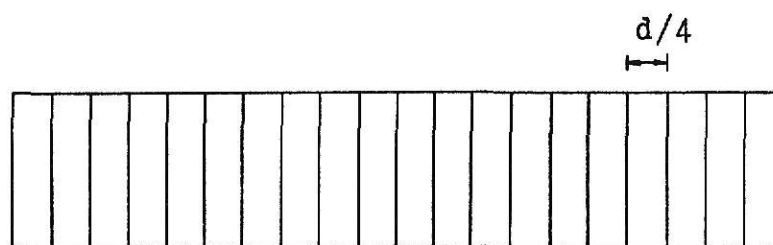
C. Discretization

It is obvious that the accuracy will improve as the size of mesh is decreased. Though no general rule can be stated as to how best dissect a given structure, the idealization is just a technique considering how the substitute structure simulates the behavior of the actual structure. Good results are frequently obtained with rather coarse subdivisions.[20] For instance, a deep rectangular beam is subjected to pure bending. Two rectangular discretizations are considered as shown in Fig. 8. We knew from assumptions of beam theory that plane cross sections remain plane in bending. However, the axial fibers of the beam become curved. Thus, in order to best approximate the straight transverse sections and curved
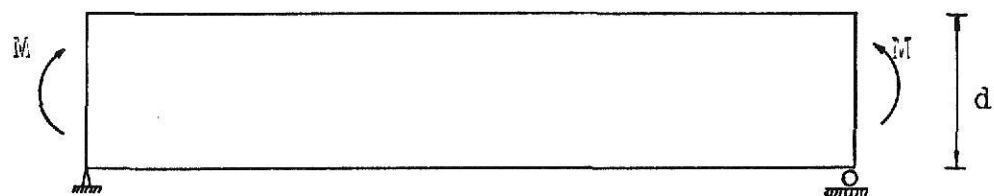
Actual Structure
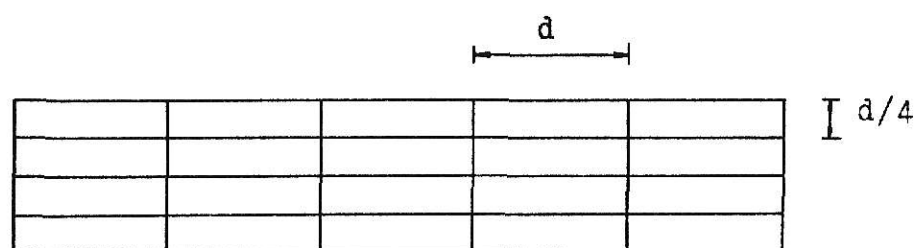
Discretization (a)

Discretization (b)

Fig. 8 Discretization of A Deep Beam

axial sections that occur during deformation, the discretization (b) in Fig. 8 is prefered over the discretization (a). Another two examples from reference (20) are shown in Fig. 9 through Fig. 12 with the surprising results shown in Fig. 9 and Fig. 11. Examination of the above typical results shows that as the triangles are well formed, i.e., essentially equilateral, better results are expected. The poorest overall displacement pattern are produced with the discretization which contains many weak triangles.

After the elements are discretized, by using a systematic procedure for numbering the nodal points, the matrix can be placed in a band form which allows the equations to be solved using a minimum of computer time and storage. The solution time is proportional to the square of band width. Fig. 13 shows that care in numbering the nodal points represents a considerable saving.[25]

Following the techniques described above, the portion to be studied in this report was discretized to be 289 elements including reinforcing members as shown in Fig. 14. Smaller triangular elements were used near the opening in order to get a better picture of stress distribution near the opening. Elements 1 to 256 are triangular plane elements. Members 257 to 275 are two force members replacing the flanges, and members 276 to 280 are also two force members representing the reinforcing bars.

D. Superposition

The boundary forces acting on the 30 in. wide plate section were
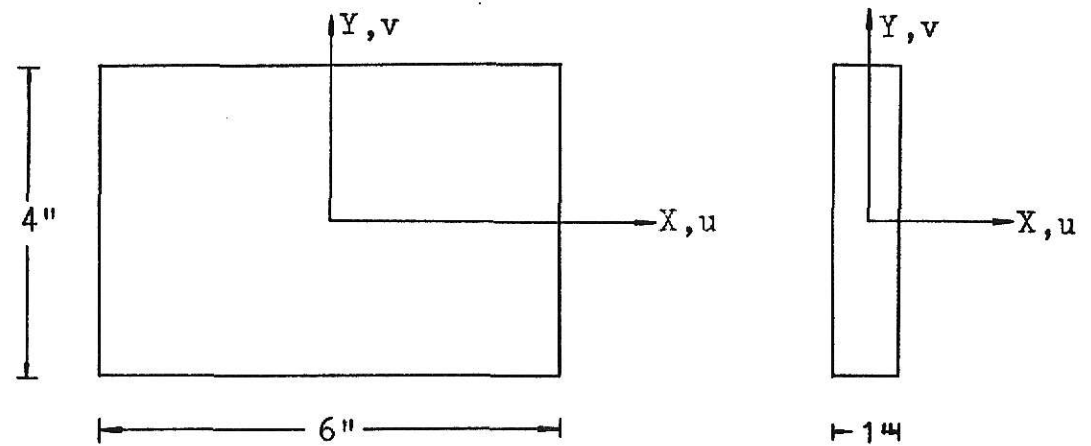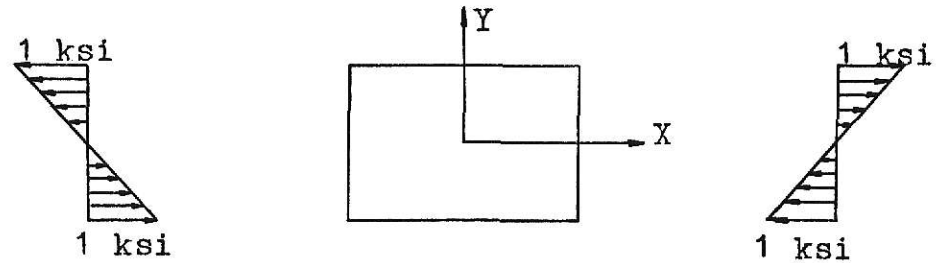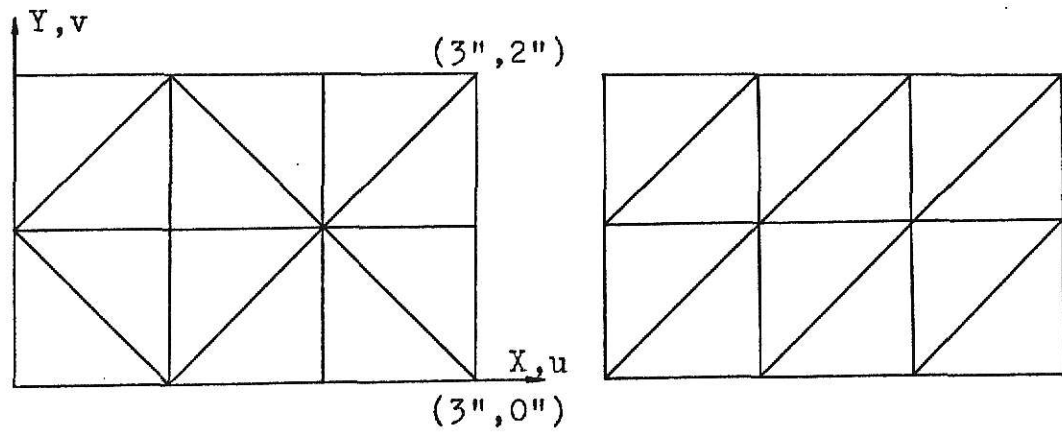
Rectangular Plate

Plate Subjected to In-plane Bending
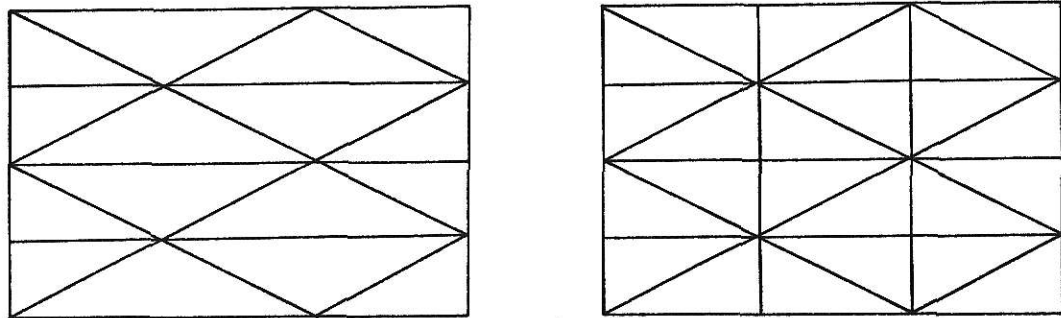
Displacements from Different Discretizations

Case	No. of Nodes	v @ x=3, y=0 F.E.M.*/Exact	u @ x=3, y=2 F.E.M./Exact
1	12	.812	.840
2	12	.916	.812
3	15	.825	.778
4	20	.919	.886
5	18	.951	.940
6	35	.960	.946

* F.E.M. = Finite Element Method

Fig. 9 Example I : Plate With Pure Bending

Fig. 10 Discretizations for Example I

Rectangular Plate

Cantilever Plate Subjected to End Shear

Displacements from Different Discretizations

Case	No. of Node	v @ x=0, y=0 F.E.M./Exact	u @ x=0, y=-2" F.E.M./Exact
1	15	.883	.836
2	23	.962	.942
3	33	.965	.950
4	45	.962	.942
5	33	.949	.912
6	45	.956	.936

Fig. 11   Example II : Cantilever Plate Subjected
          to End Shear

Case 1 : 15 Nodes 16 Elements   Case 2 : 23 Nodes 32 Elements

Case 3 : 33Nodes 48 Elements   Case 4 : 45 Nodes 64 Elements

Case 5 : 33 Nodes 44 Elements   Case 6 : 45 Nodes 60 Elements

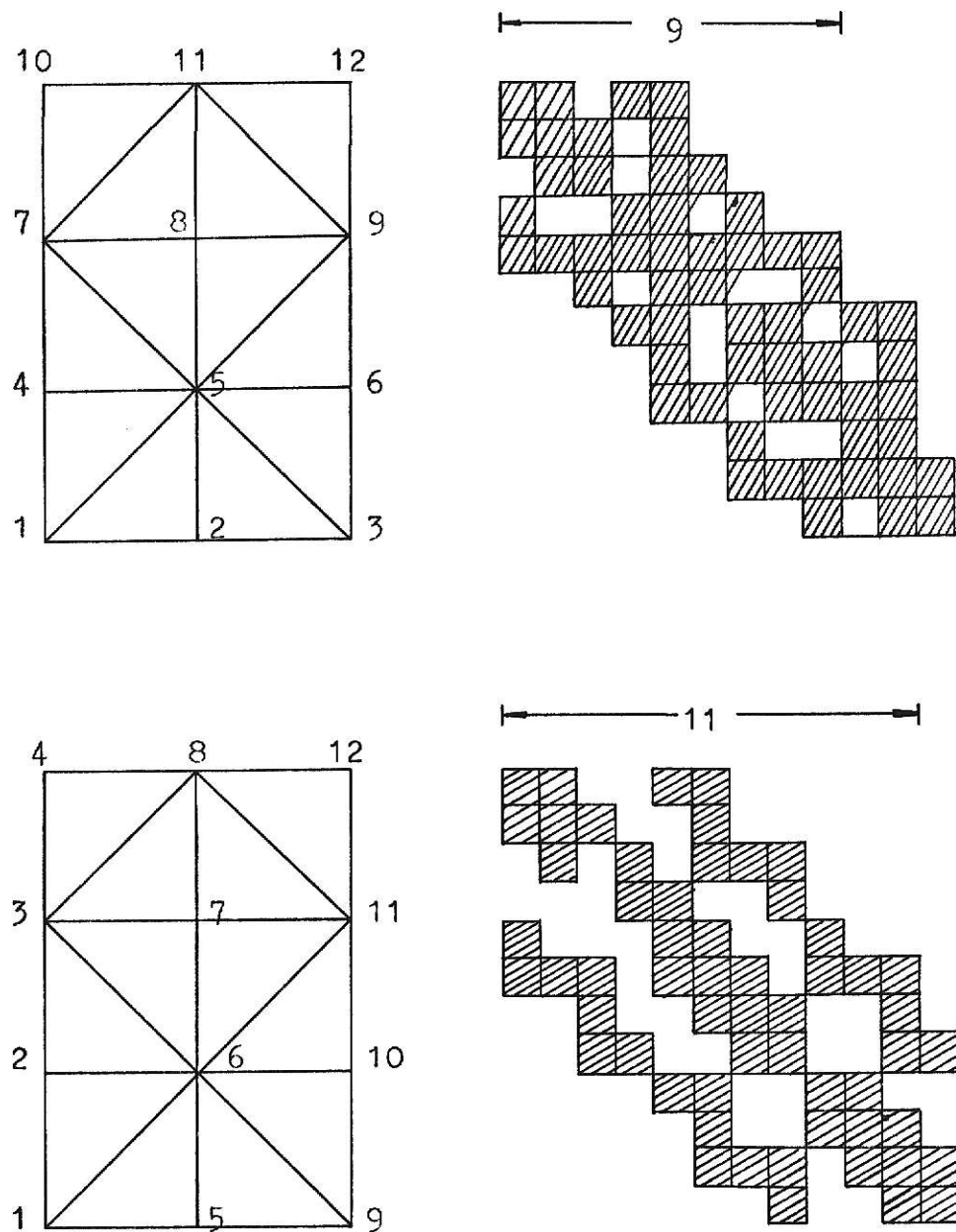Fig. 12 Discretizations for Example II

Fig. 13 The Effect of The Nodal Point Numbering
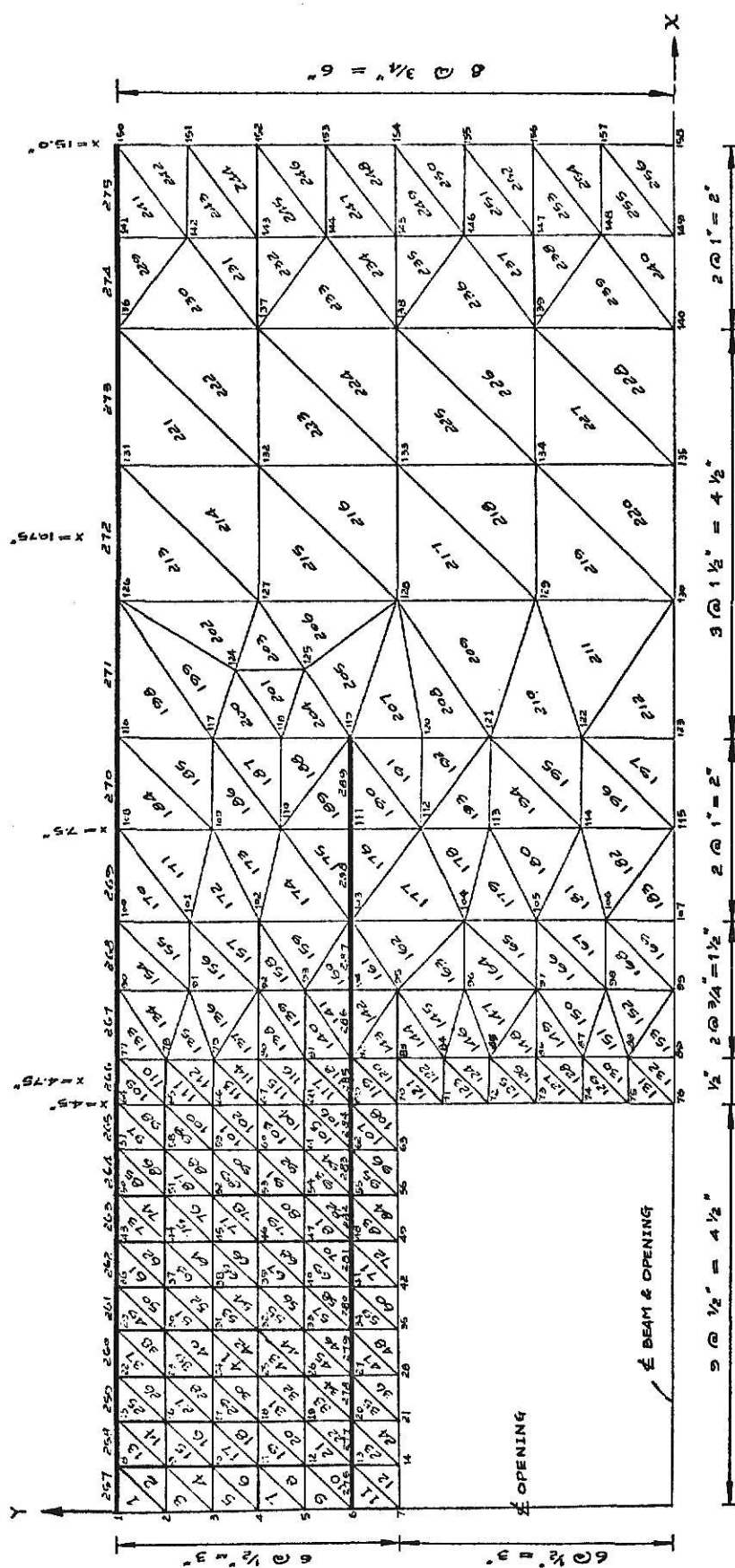System on The Band Width of The Stiffness
Matrix

Fig. 14 Finite Element Discretization for the Report

regarded as made up of two different forces as shown in Fig. 15. The isolated portion subjected to end shears and moments is statically equivalent to the same portion subjected to a pure bending plus shear with bending. By static equilibrium, the factors X_1 and X_2 can be found for any shear-moment combination by solving the following two equations simultaneously

$$1000 \, X_1 - 1000 \, X_2 = M_A$$

$$1000 \, X_1 + 1000 \, X_2 = M_B$$

Four sets of X values for different moment-shear ratios are listed in the table in Fig. 15.

(a). Displacement Boundary Condition

Due to the pure bending, Fig. 16(a), the portion is symmetrical with respect to the Y axis and antisymmetrical with respect to the X axis. For the case of bending with shear, the portion is antisymmetrical with respect to both the X and Y axes. Therefore it was possible to analyze only one-quarter of the section by introducing appropriate restraint conditions on the boundary nodes as illustrated in Fig. 16(b) and Fig. 16(c).
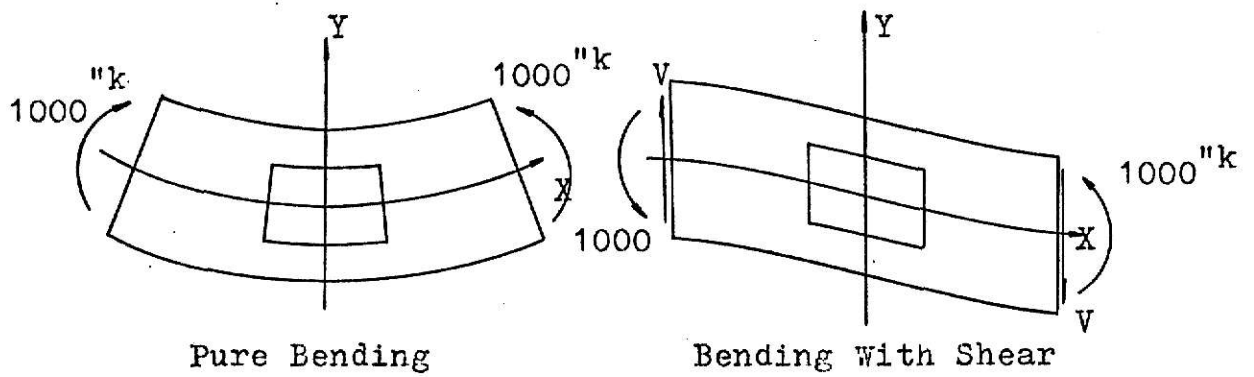
(b). Consistent Nodal Loads

The moments and shear forces on the free body shown in Fig. 16 were approximately represented by a series of concentrated loads applied at the nodal points on the end section in this analysis. The bending stresses at the end section were calculated by means of the flexural formula
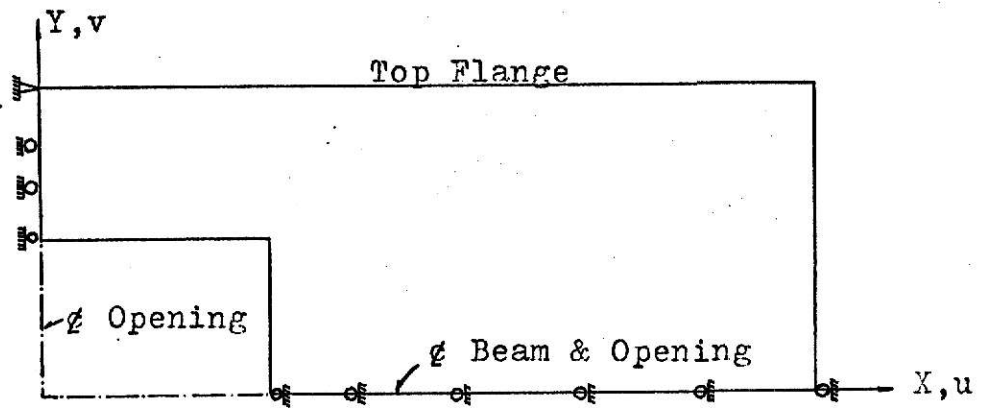
Pure Bending

End Shear With Bending
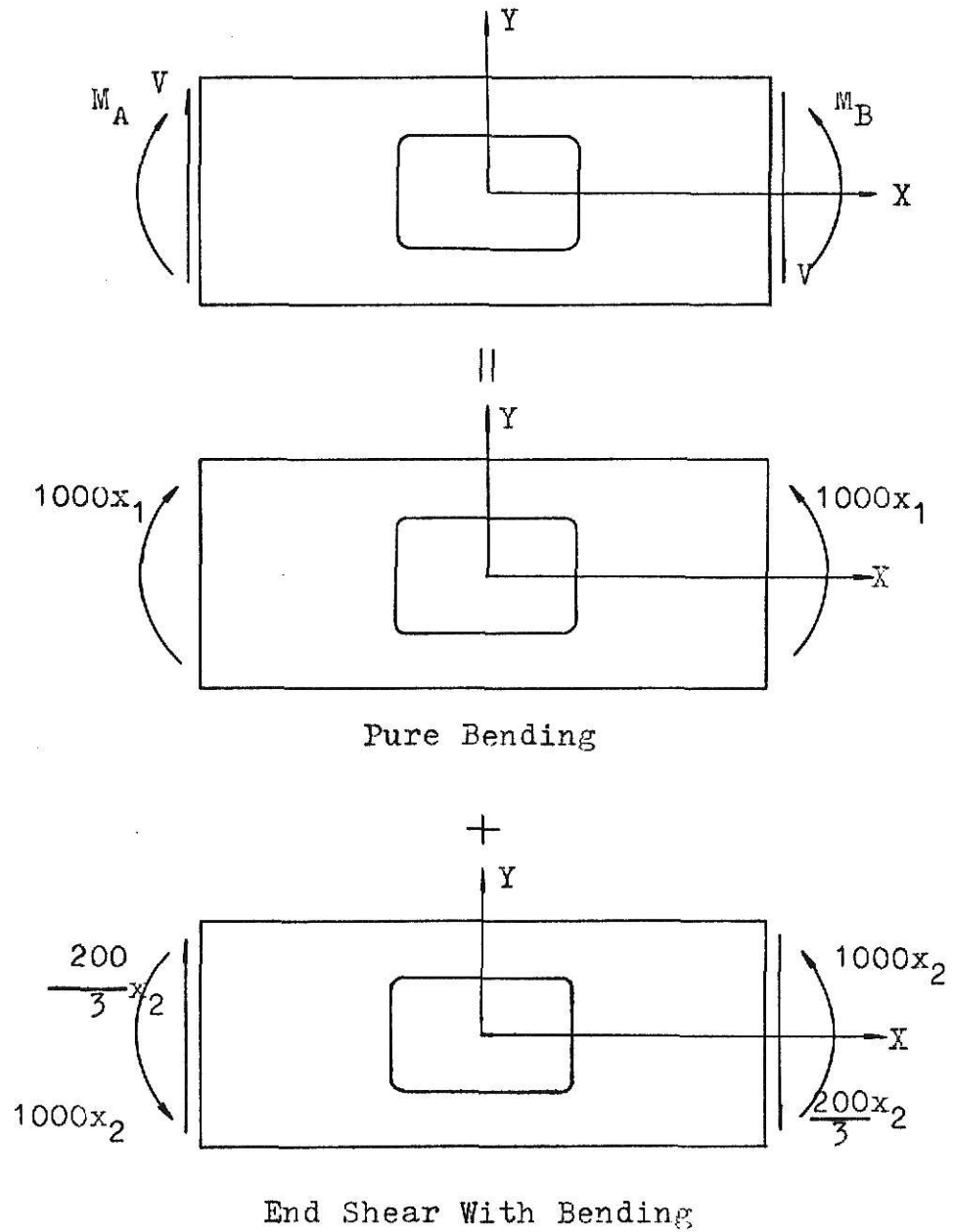
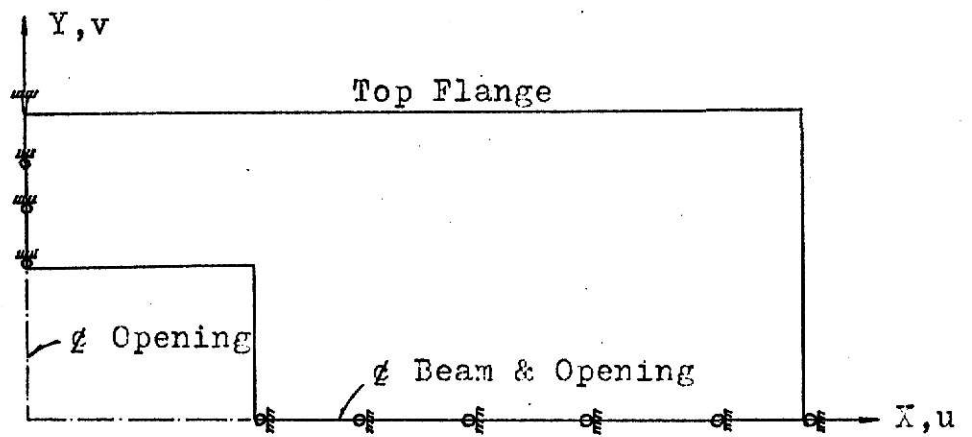| M/V	M_A	M_B	x_1	x_2	V
80	780	1140	0.96	0.18	$200x_2/3$
60	540	900	0.72	0.18	$200x_2/3$
40	300	660	0.48	0.18	$200x_2/3$
20	60	420	0.24	0.18	$200x_2/3$

Fig. 15 Superimposed Loading Conditions
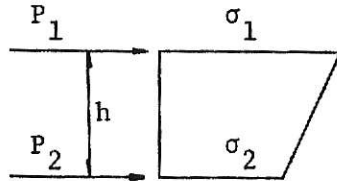
a. Deformation Shape

b. Pure Bending

c. End Shear With Bending

Fig. 16   Displacement Boundary Conditions

$$\sigma = \frac{Mc}{I}$$

Since the stress varies linearly along the boundary, the consistent nodal loads were found by the trapezoidal loading formula

$$P_1 = \frac{ht}{6} (2\sigma_1 + \sigma_2)$$

$$P_2 = \frac{ht}{6} (\sigma_1 + 2\sigma_2)$$

t = thickness of web

σ = force intensity per unit area

The concentrated load at each nodal point was the sum of the static resultants from the adjacent sides. The small difference between the sum of the moments produced by these concentrated nodal loads about the neutral axis and the statical moment at the section was proportionately resolved into a series of small concentrated loads, which were then added to the previous concentrated loads. The sum of the moments produced by these resultant concentrated loads were equal to a half of the statical moment 1000 K-in. The concentrated loads are shown in Fig. 17.

The shearing stresses were calculated by the formula

$$v = \frac{VQ}{bI}$$

The consistent nodal loads from the resultant of parabolic variation loading were calculated by the formula
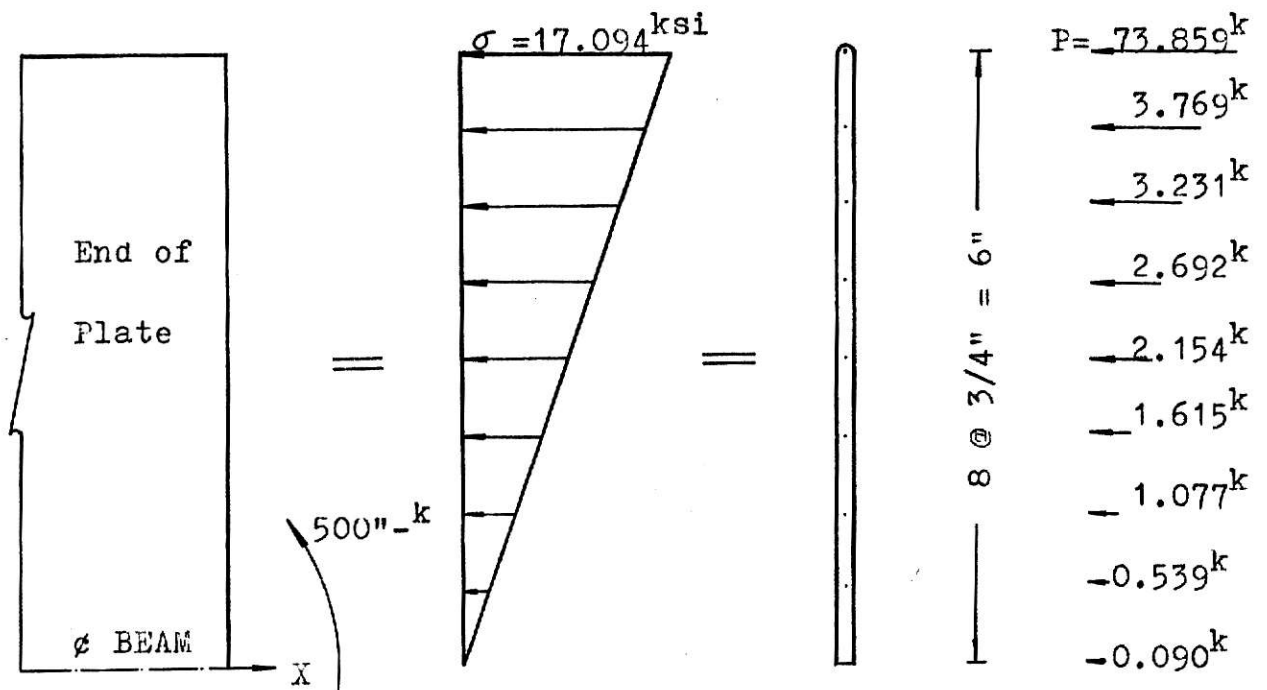
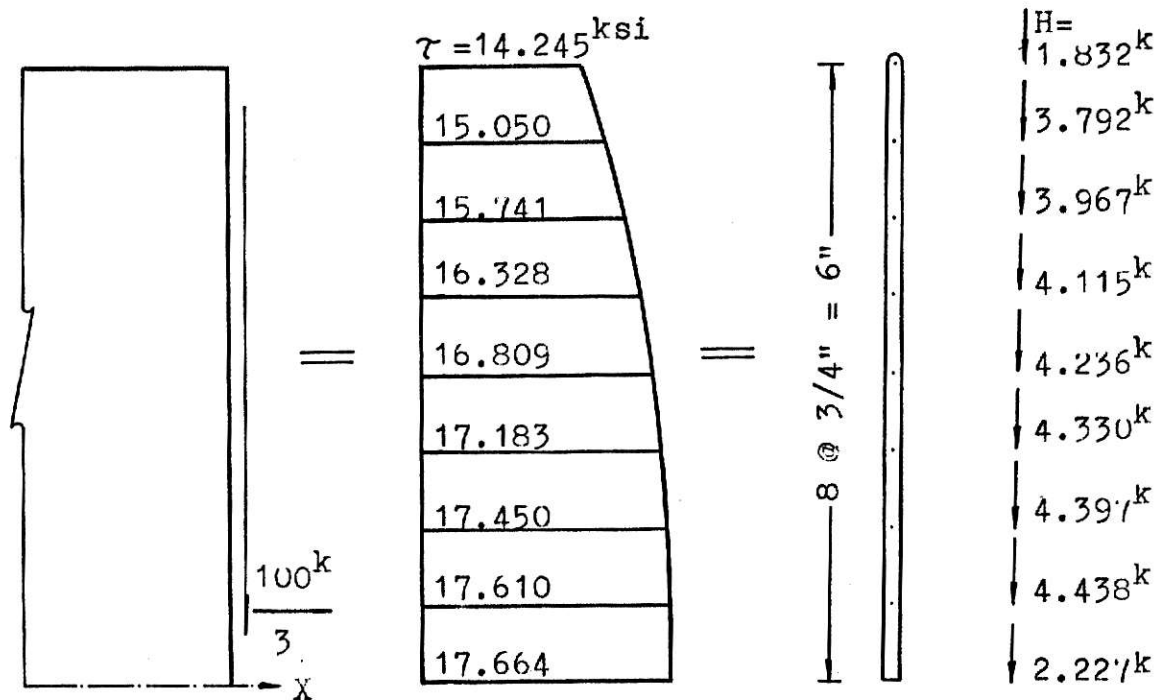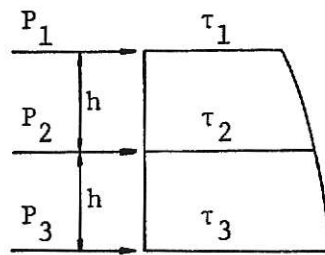Fig. 17   Consistent Nodal Loads for Pure Bending

Fig. 18   Consistent Nodal Loads for End Shear

$$P_1 = \frac{th}{24} (7\tau_1 + 6\tau_2 - \tau_3)$$

$$P_2 = \frac{th}{12} (\tau_1 + 10\tau_2 + \tau_3)$$

τ_i = shear stress per unit area

t = thickness of web

The shear stress on the flange was assumed to be concentrated at the center point of the flange. The consistent nodal loads are shown in Fig. 18.

V. PRESENTATION AND COMPARISON OF RESULTS

The stresses determined by the finite element method using constant strain triangles are constant throughout an element. Two basic approaches have evolved for the interpretation of the stresses. Provided that the material properties of the elements on a node are the same, the corresponding stresses in these elements may be averaged and the result attributed to the common node. Alternatively, the stresses determined for an element may be assigned to a particular point within the element — usually the centroid. In this report the second procedure was used to determine the stress distribution.

A. Normal Stresses

In Fig. 19 through Fig. 22, the normal stresses were calculated by the finite element method were compared with the stresses calculated by the Vierendeel method and the experimental results in reference (3). The stresses at section x = 0 and x = -4.5" for a 4" extension of reinforcing were compared with the experimental results. Four setups of different M/V ratio were plotted. The solid line represents the results of the finite element method with the calculated values at cross points.

It is seen that the finite element method agrees better with the experimental results than the Vierendeel method at the centerline of the opening (X = 0). At the section X = -4.5", the normal stresses are not all in good agreement with the experimental results. However, the finite element method appears to predict a more reasonable stress distribution than the Vierendeel method which, unlike the elasticity analysis, predicts linear bending stresses and does not account for stress concentration. For all cases, the finite element method predictions are in

excellent agreement with the experimental values for the stresses at
flanges.

Using the same cross section and the same location of reinforcing
bar, the different stress distribution for different lengths of rein-
forcing are shown in Fig. 23 through Fig. 26. The results for no re-
inforcement and the 6" extension of reinforcing were from a report
by Y.I. Hsu[26] at Kansas State University. At the section X = 0, the
stress at the top edge of opening for the 2" extension of reinforcing
was found to be 50% of the corresponding stress with no reinforcing,
and the stress for the 6" extension of reinforcing was about 68% of
the corresponding stress with no reinforcing. These are shown in
Figs. 23a, 24a, 25a, and 26a. In Figs. 23c, 24c, 25c, and 26c, at the section
X = - 4.75", the stress for the 2" extension case is about 90% of the
stress for the unreinforced case, while the stress for the 6" extension
case is only 70% of the stress for the unreinforced case. The graphs
at the section X = - 10.75" show that the stress distribution is only
slightly affected by the opening. The stress distribution patterns are
similar for the four cases of M-V. However, the magnitude of the
stresses are unusual and interesting. The case with no reinforcement
has the smaller stress of the four cases, while the 4" extension case
has a larger stress than other three cases. The reason the maximum
stress with the 4" extension is larger than the maximum stress with the
6" extension at the section X = -10.75" is evident. When the reinforcing
was terminated near a section, only the local stress concentration occured,

and the average stress for the calculated area tended to be low.

B. Shear Stresses

The results of the experiments[3] indicated that the shear stress distribution was insensitive to the M-V ratio. The shear stresses for an M-V ratio of 60" were plotted to represent the results for the series.

In Fig. 27, the shear stresses at sections X = 0, X = - 7.5", and X = - 10.75" were shown for the 4" extension of the reinforcing. The results of both the Vierendeel method and the experimental data were from reference 3 and compared with the results of the finite element method. It can be seen that the predictions based on the finite element method were in excellent agreement with the experimental results. The results evaluated from the Vierendeel method indicated a linear stress distribution which tended to correspond to the mean value obtained from the finite element method except at the section X = 0.

In Fig. 28, the shear stresses for different lengths of reinforcing were compared using the finite element analysis. The M-V ratio of 60" was used to represent the series. The shear stresses are not much difference except at the location near the reinforcing terminal.
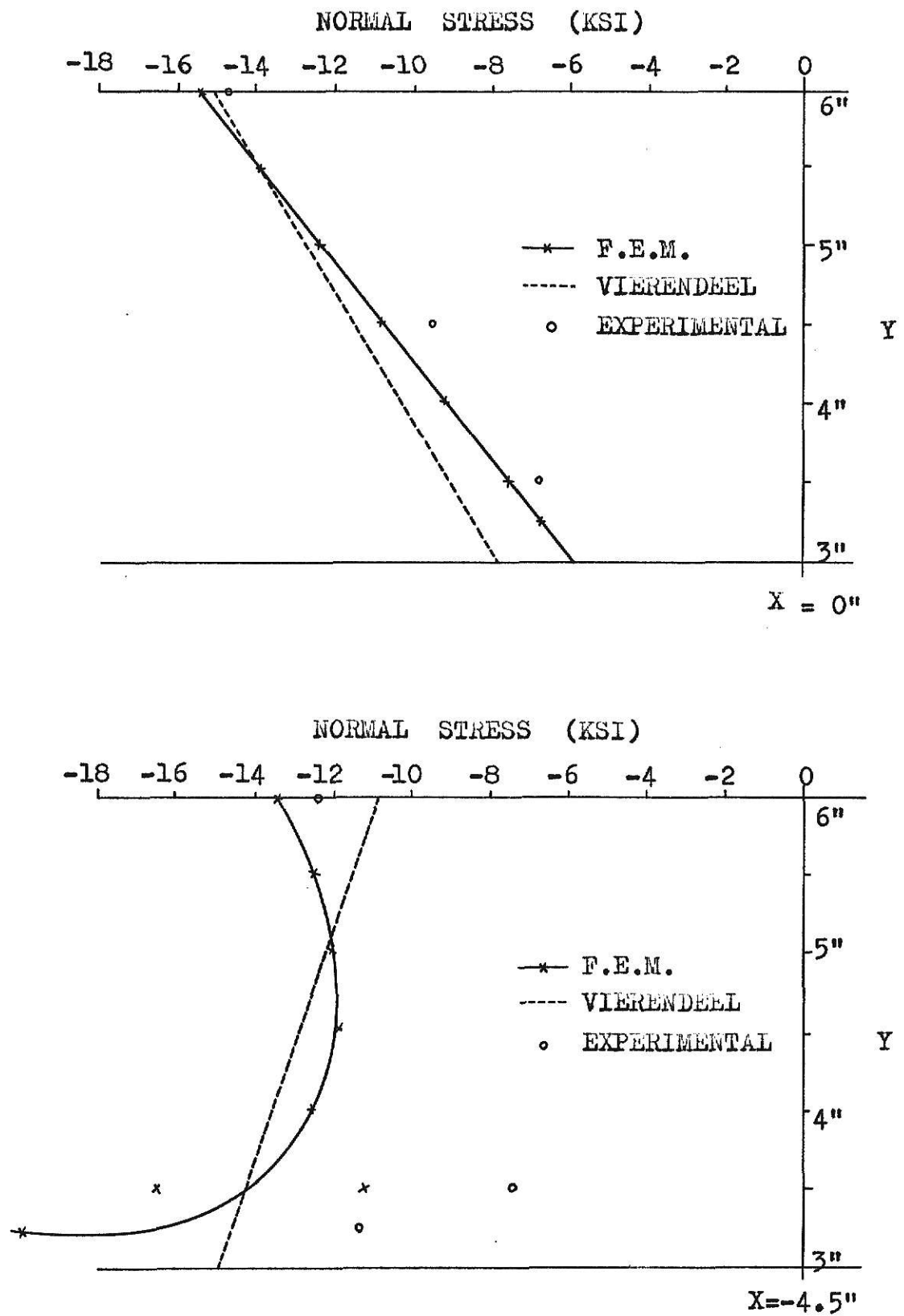
NORMAL STRESS (KSI)

-18 -16 -14 -12 -10 -8 -6 -4 -2 0

6"

—×— F.E.M.

----- VIERENDEEL

o EXPERIMENTAL

Y

5"

4"

3"

X = 0"

NORMAL STRESS (KSI)

-18 -16 -14 -12 -10 -8 -6 -4 -2 0

6"

—×— F.E.M.

----- VIERENDEEL

o EXPERIMENTAL

Y

5"

4"

3"

X = -4.5"

Fig. 19 Normal Stresses From Different Approaches

For M/V = 80"

NORMAL STRESS (KSI)

-18   -16   -14   -12   -10   -8   -6   -4   -2   0

—×— F.E.M.

----- VIERENDEEL

∘ EXPERIMENTAL

Y

X = 0

NORMAL STRESS (KSI)

-20   -18   -16   -14   -12   -10   -8   -6   -4   -2

—×— F.E.M.

----- VIERENDEEL

∘ EXPERIMENTAL

Y

X = -4.5"

Fig. 20 Normal Stresses From Different Approaches

For M/V = 60"

NORMAL STRESS (KSI)

-18 -16 -14 -12 -10 -8 -6 -4 -2 0

6"

×—— F.E.M.
---- VIERENDEEL
○ EXPERIMENTAL

Y

5"

4"

3"

X = 0

NORMAL STRESS (KSI)

-18 -16 -14 -12 -10 -8 -6 -4 -2 0

6"

×—— F.E.M.
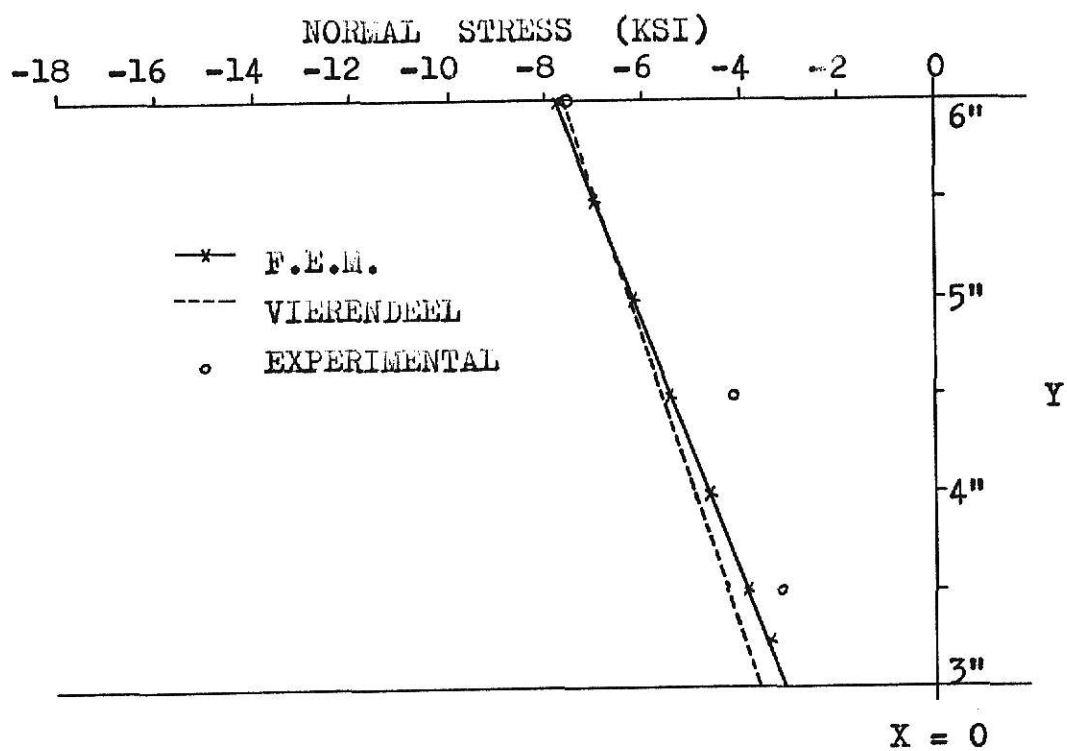---- VIERENDEEL
○ EXPERIMENTAL

Y

5"

4"

3"

X = -4.5"
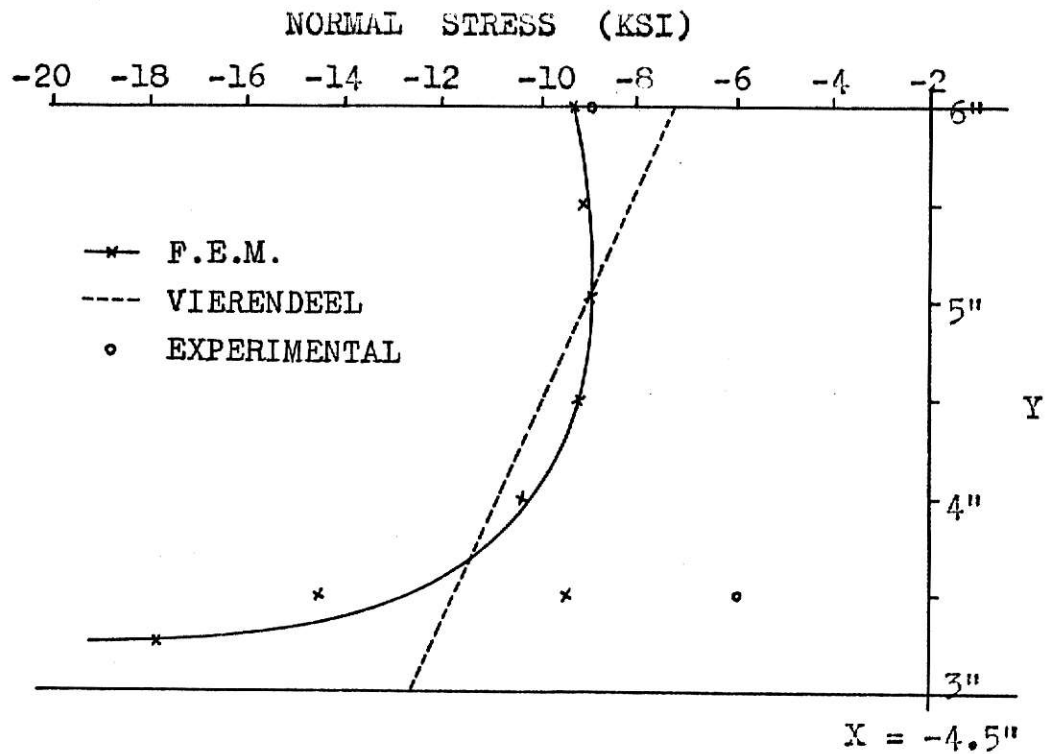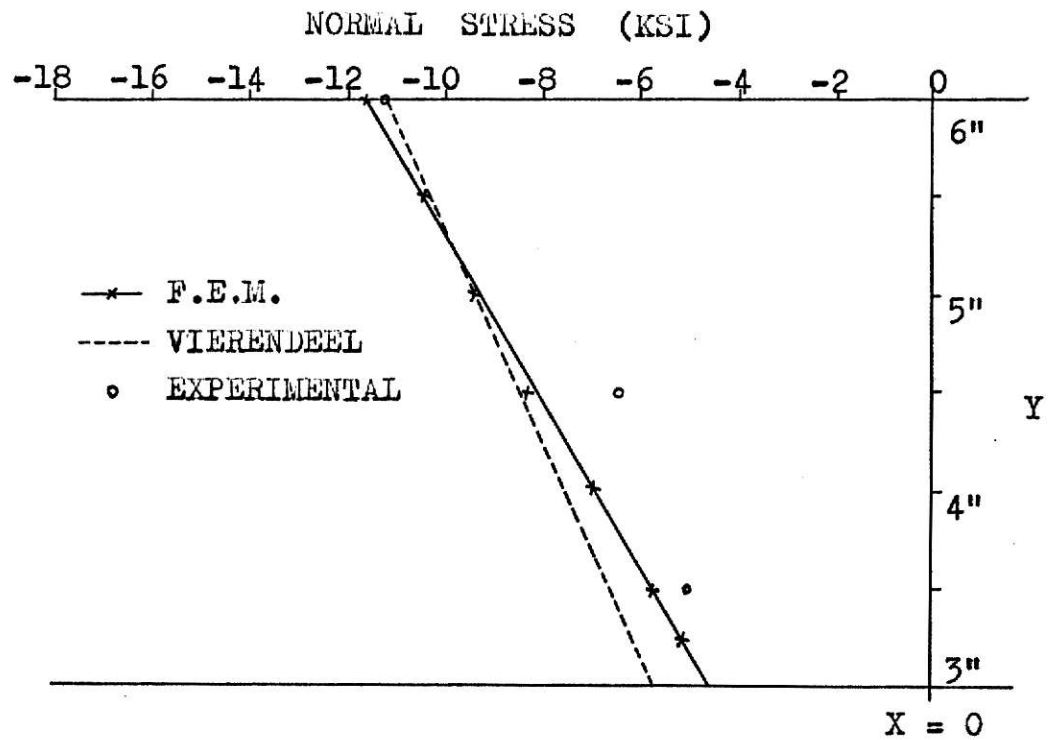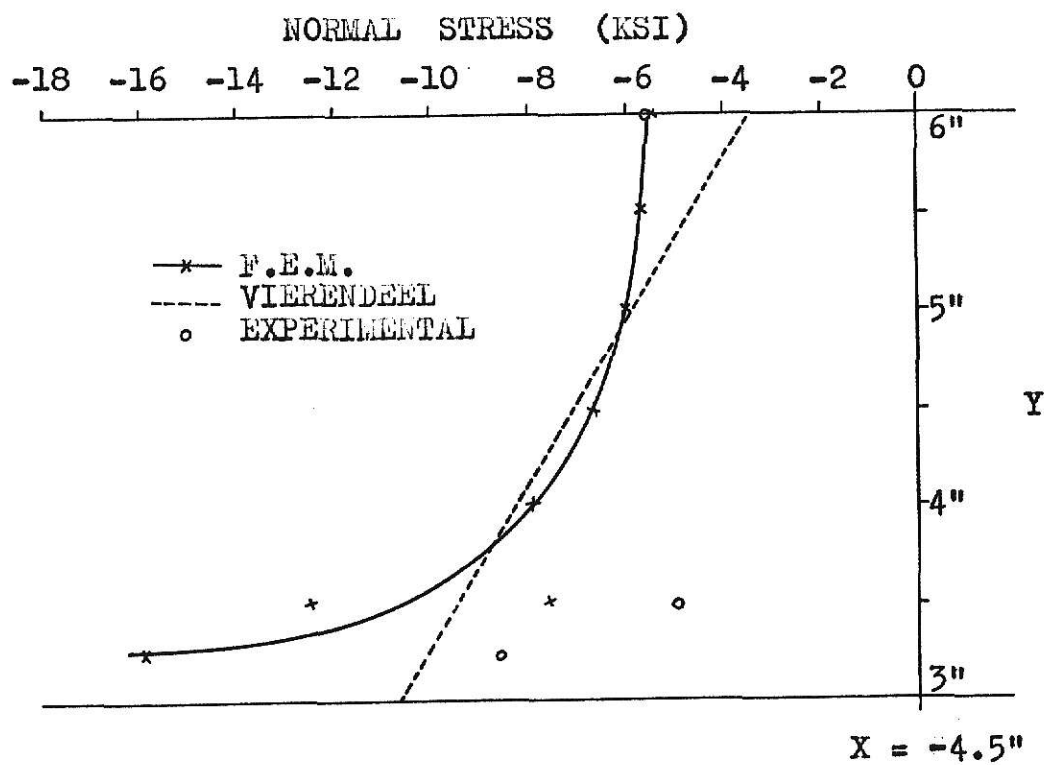
Fig. 21 Normal Stresses From Different Approaches

For M/V = 40"

ILLEGIBLE DOCUMENT

THE FOLLOWING
DOCUMENT(S) IS OF
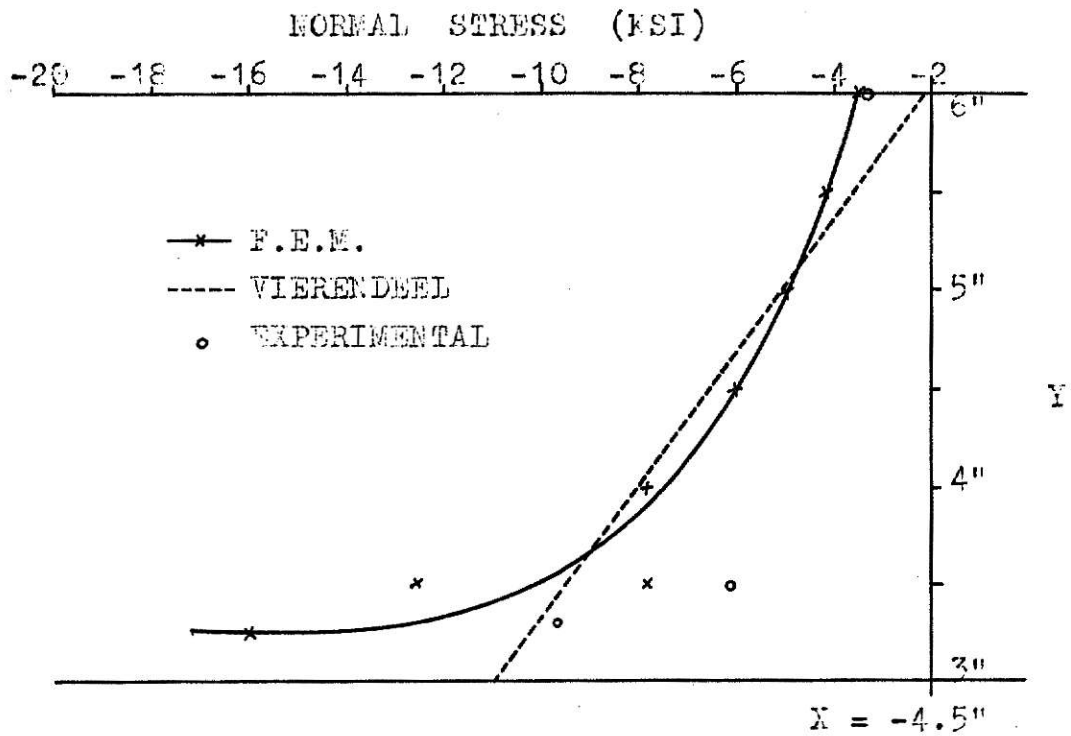POOR LEGIBILITY IN
THE ORIGINAL

THIS IS THE BEST
COPY AVAILABLE

P-474
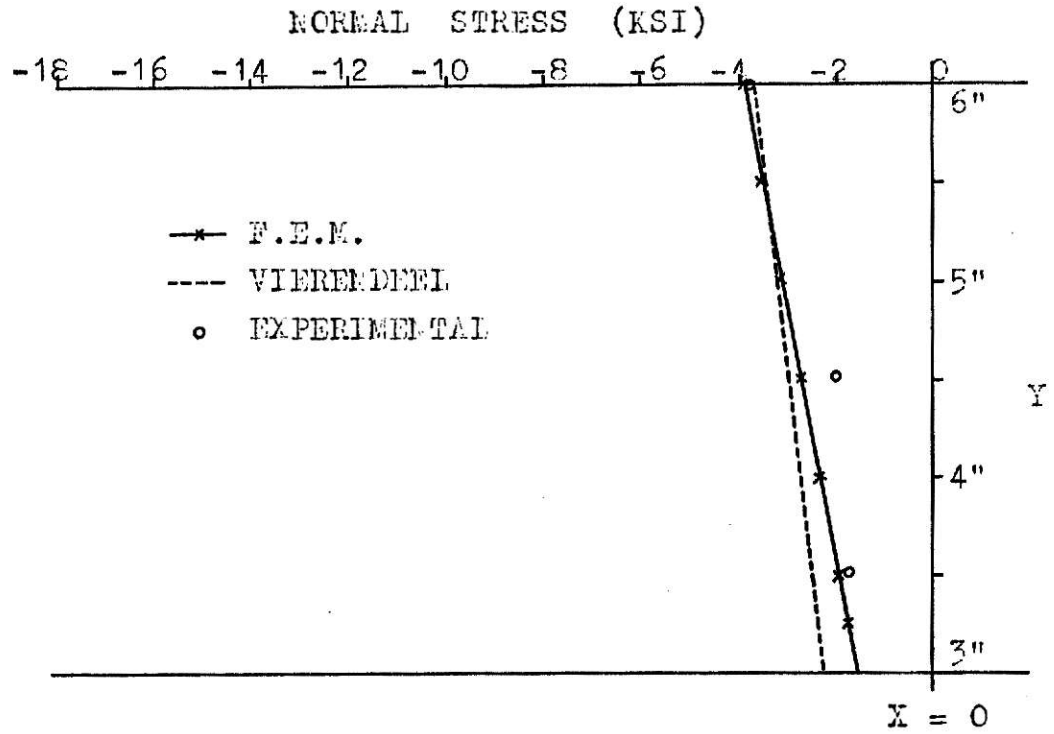
NORMAL STRESS (KSI)

Fig. 22 Normal Stresses From Different Approaches
For M/V = 20"

NORMAL STRESS (KSI)

-18   -16   -14   -12   -10   -8   -6   -4   -2   0

2"Extension

Unreinforced

6"   4"

Y

6"
5"
4"
3"

Fig. 23a   x = 0

NORMAL STRESS (KSI)

-28   -26   -24   -22   -20   -18   -16   -14   -12   -10

Unreinforced

6"Extension

2"

4"

Y

6"
5"
4"
3"
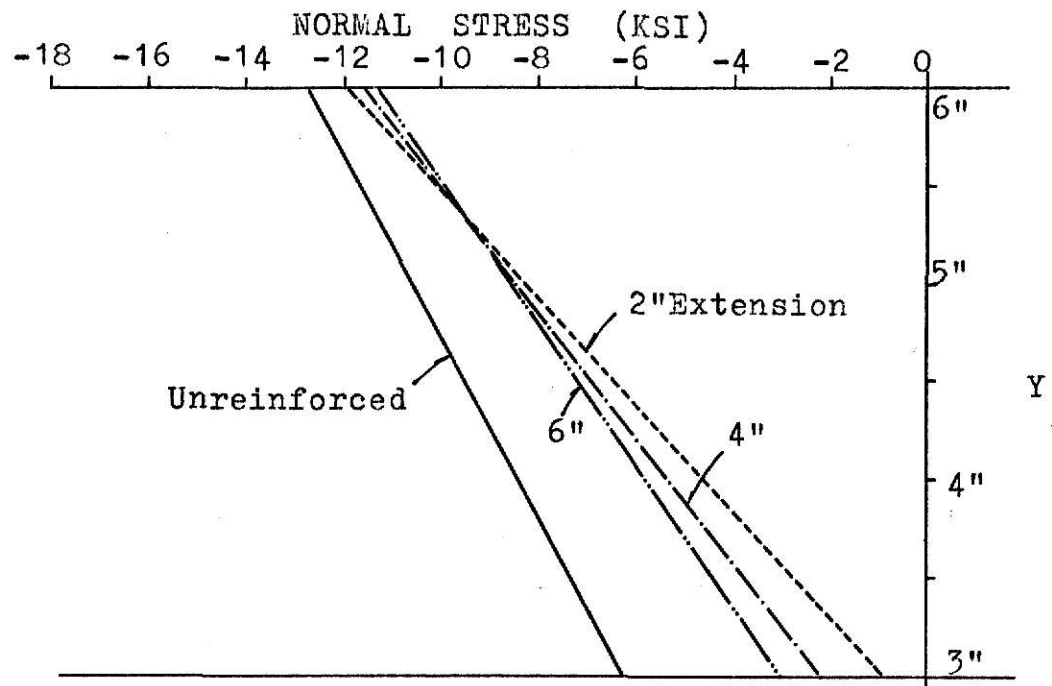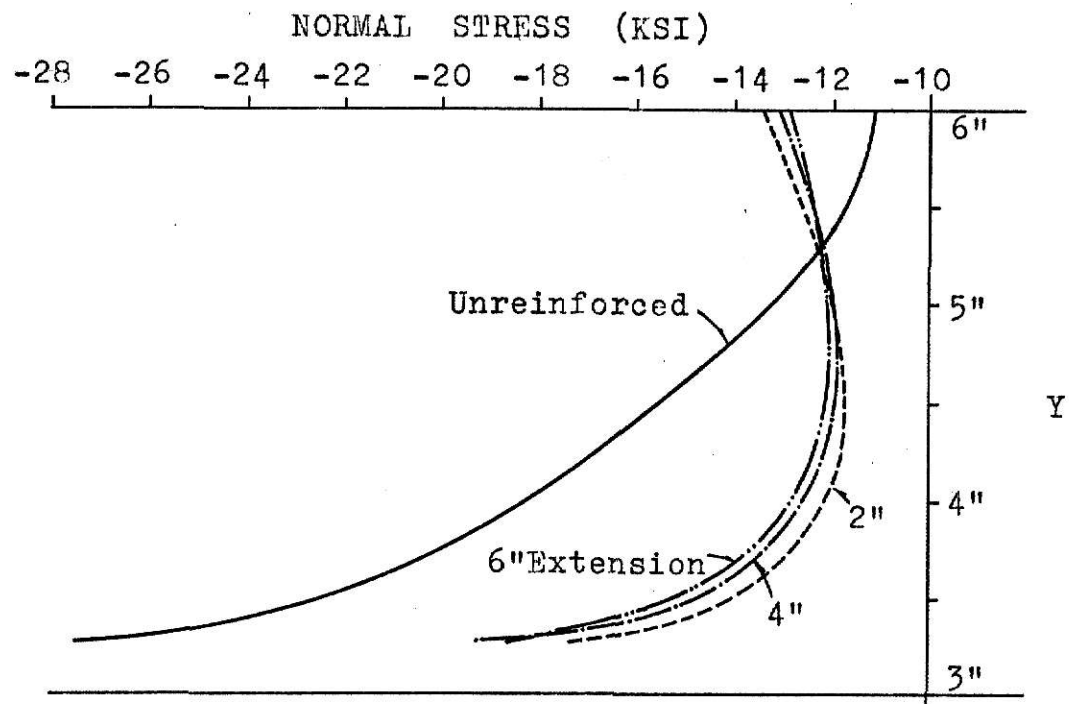
Fig. 23b   x = -4½"

Fig. 23   Effects of Reinforcement on Normal Stresses
For M/V = 80"

NORMAL STRESS (KSI)

-24 -22 -20 -18 -16 -14 -12 -10 -8 -6 -4

Unreinforced

2"Extension

4"

6"Extension

6"

5"

Y

4"

3"

Fig. 23c x = -4.75"

NORMAL STRESS (KSI)

-22 -20 -18 -16 -14 -12 -10 -8 -6 -4 -2

6"

Unreinforced

6"

4"

2"Extension

5"

Y

4"

3"

Fig. 23d x = -7½"

NORMAL STRESS (KSI)

-18 -16 -14 -12 -10 -8 -6 -4 -2 0

6"

Y

5"

Unreinforced

2"

4"Extension

4"

6"

3"

Fig. 23e   x = $-10^3/4$"

NORMAL STRESS (KSI)

-18 -16 -14 -12 -10 -8 -6 -4 -2 0

6"

Y

5"

2"Extension

Unreinforced   6"

4"

4"

3"
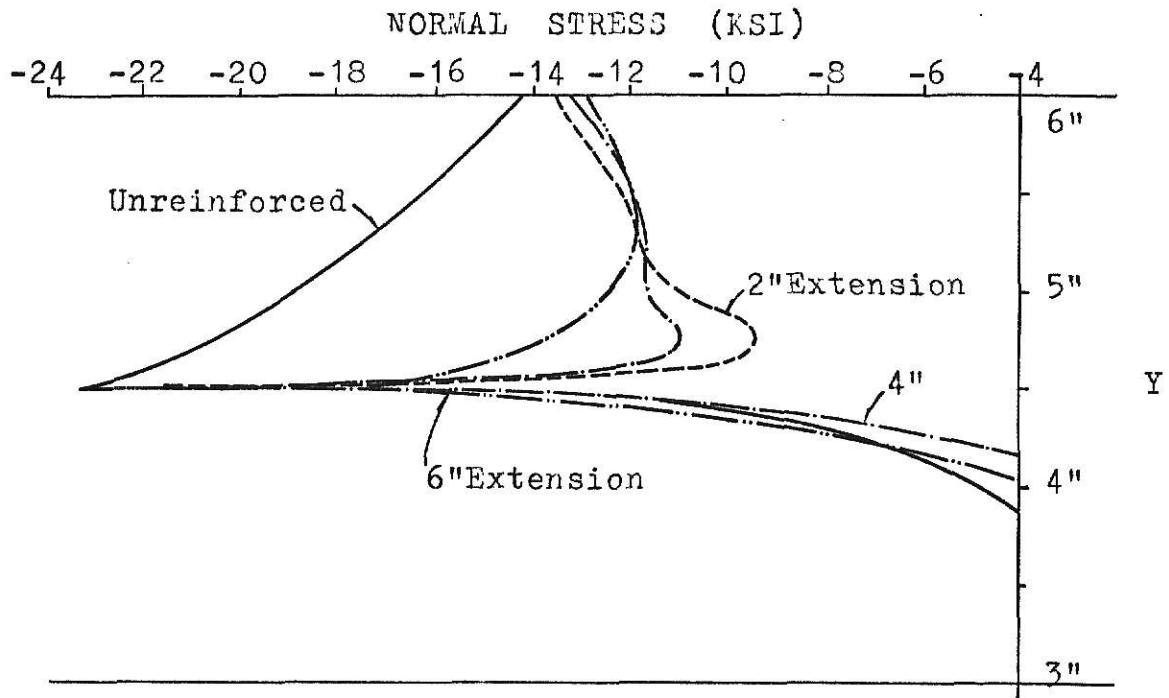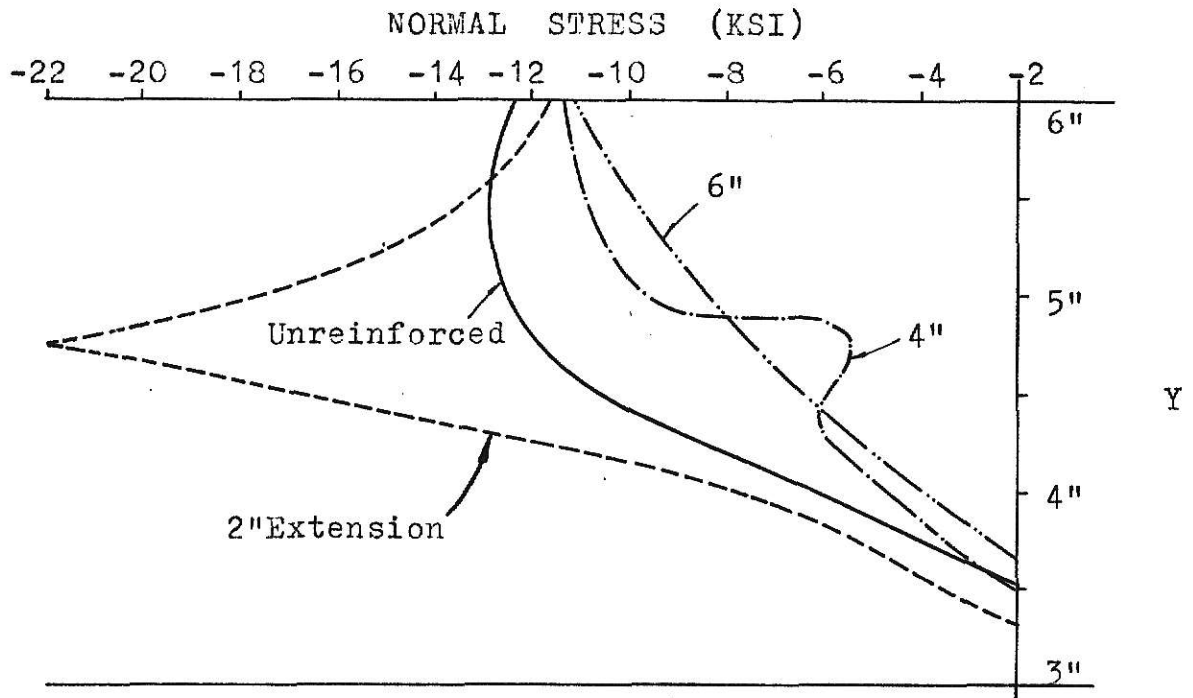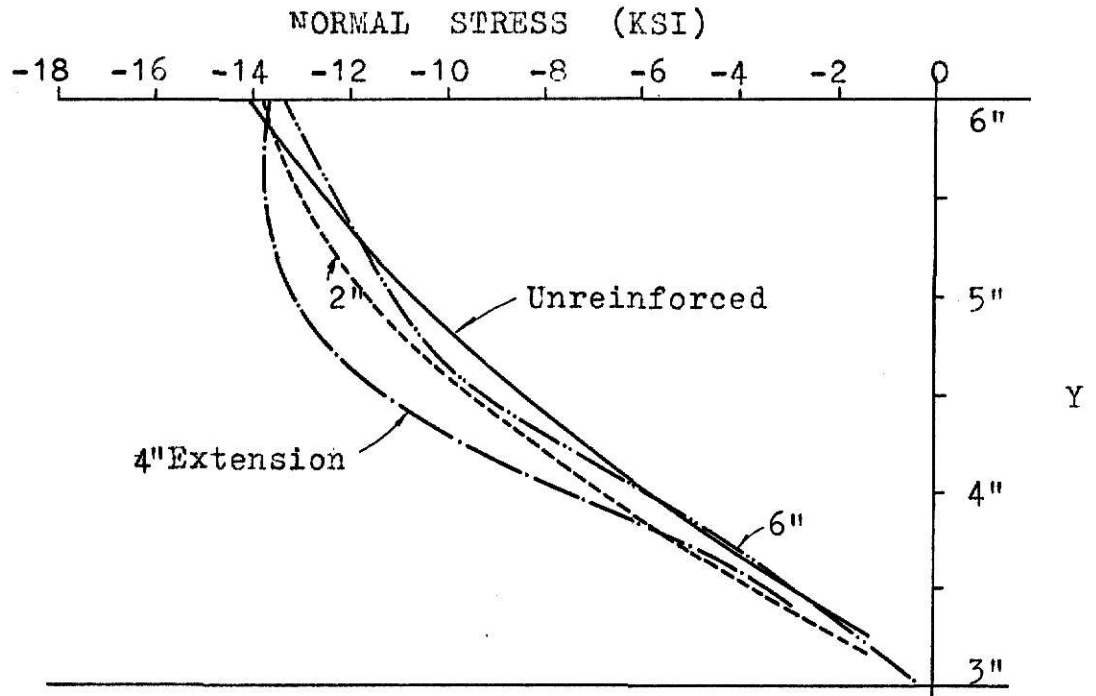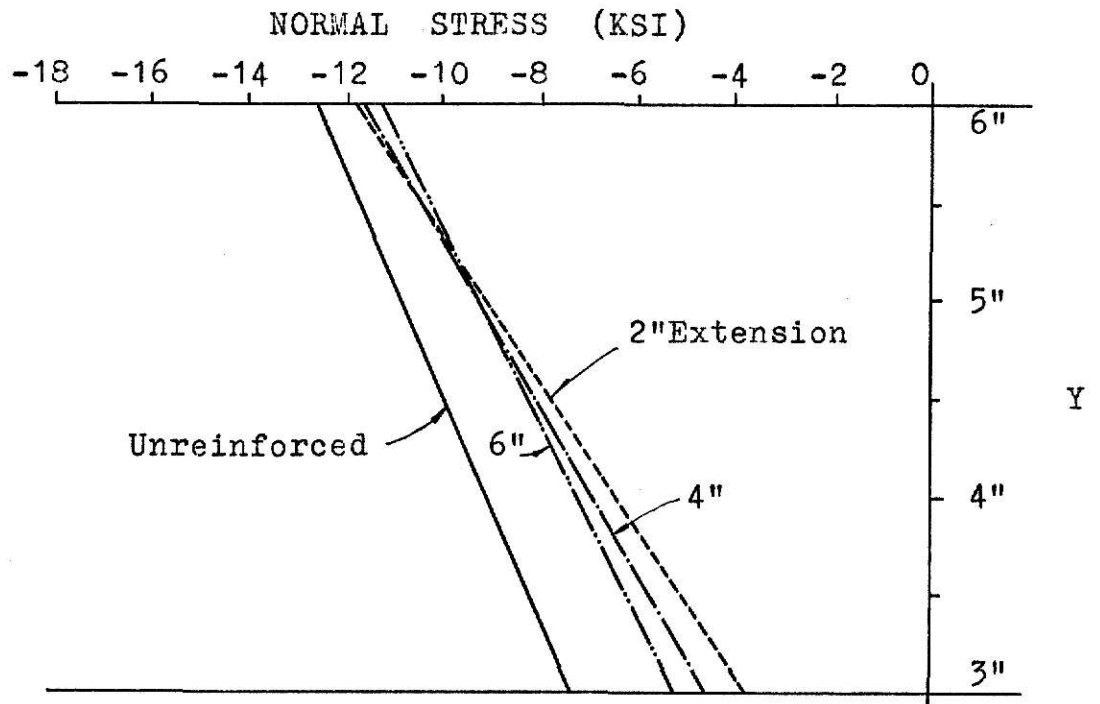
Fig. 24a   x = 0

Fig. 24   Effects of Reinforcement on Normal
Stresses for M/V = 60"

NORMAL STRESS (KSI)

-24 -22 -20 -18 -16 -14 -12 -10 -8 -6

6"

Unreinforced

5"

Y

4"

4"

6"Extension

2"

3"

Fig. 24b x = -4½"

NORMAL STRESS (KSI)

-24 -22 -20 -18 -16 -14 -12 -10 -8 -6
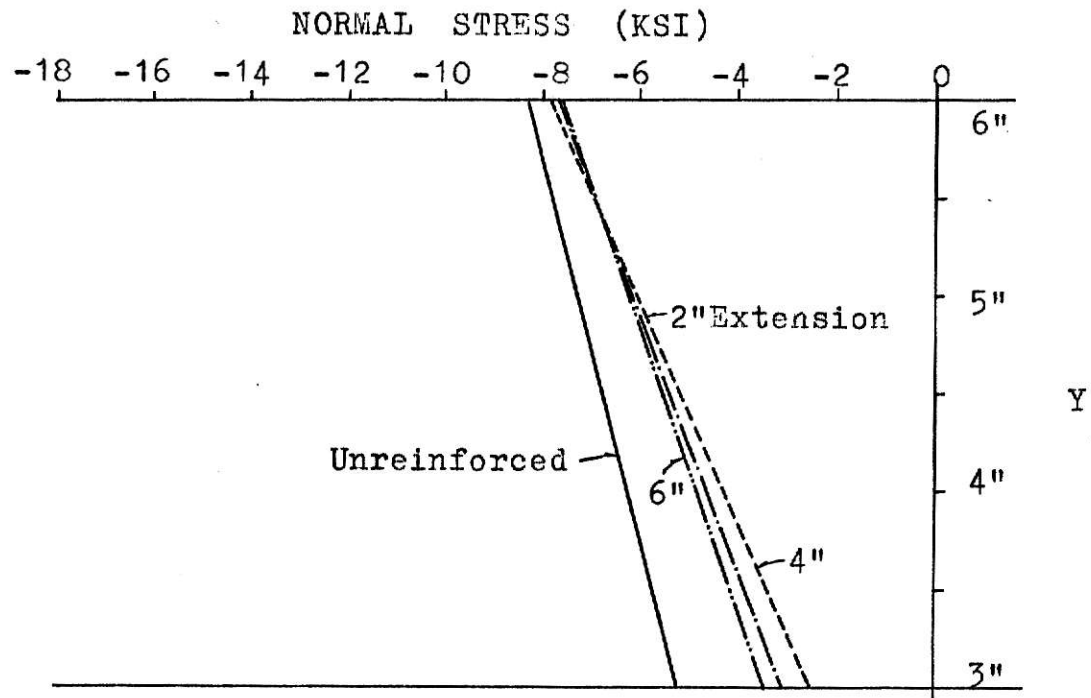
6"

5"

4"

4"

6"Extension

2"

3"

Y

Unreinforced

2"

1"

0

Fig. 24c x = -4³/4"

NORMAL STRESS (KSI)

-18 -16 -14 -12 -10 -8 -6 -4 -2 0

6"
5"
4"
3"   Y
2"
1"
0

6"   4"

2"Extension

Unreinforced

Fig. 24d   x = -7½"

NORMAL STRESS (KSI)

-18 -16 -14 -12 -10 -8 -6 -4 -2 0

6"
5"
4"
3"   Y
2"
1"
0

Unreinforced

4"Extension

6"

2"
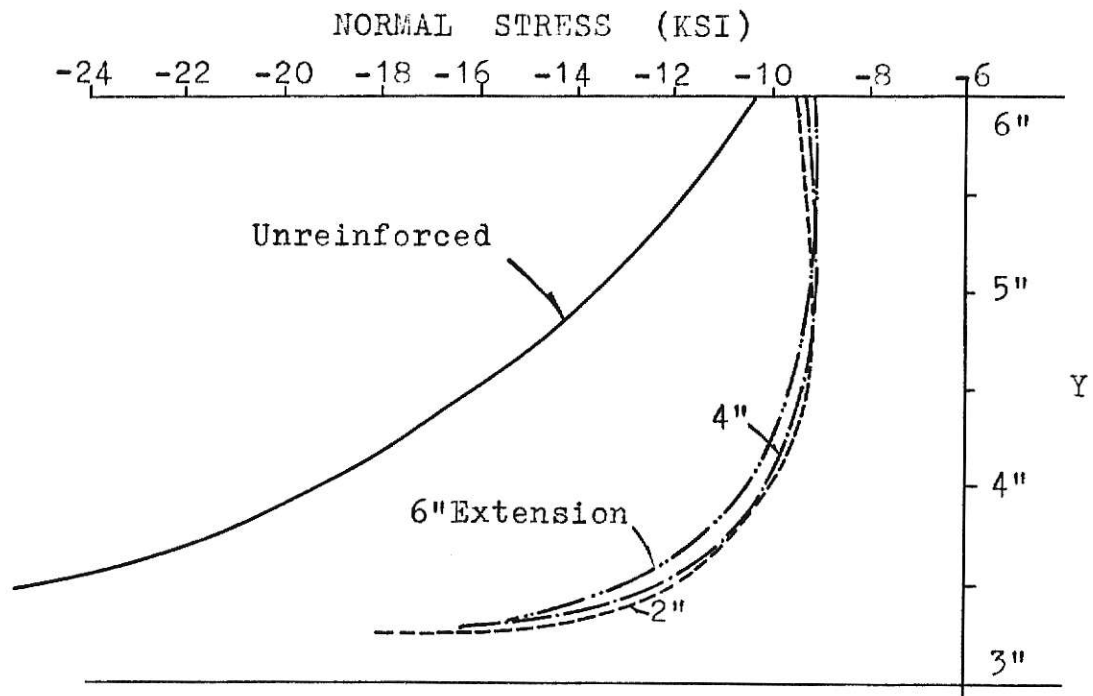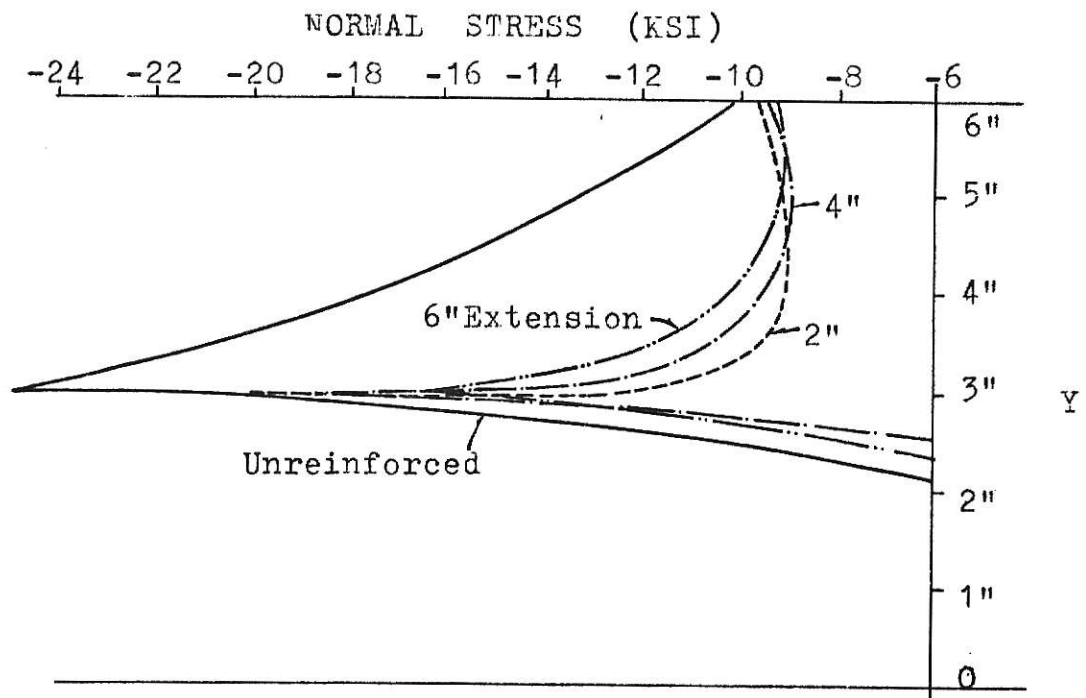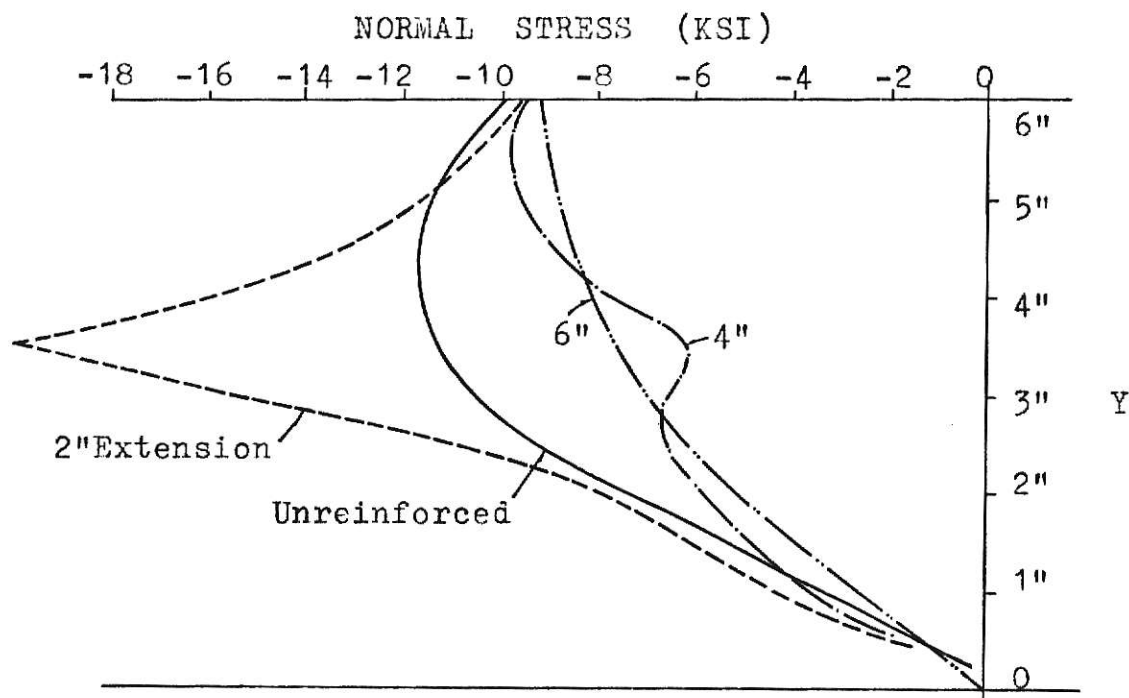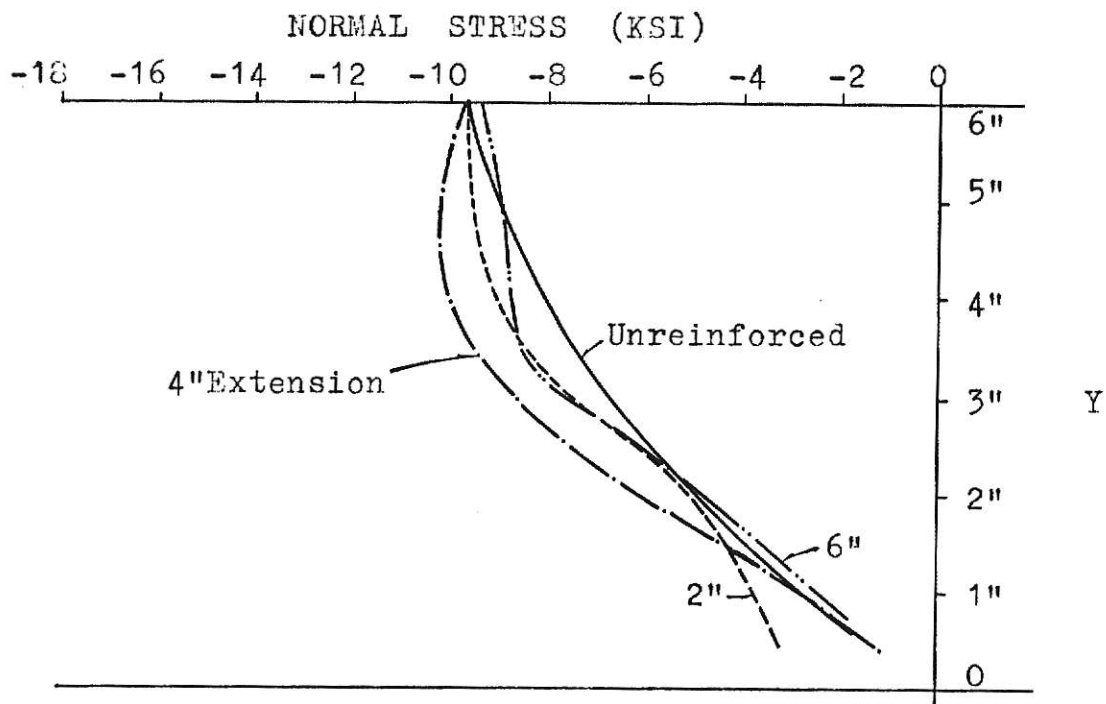
Fig. 24e   x = -10³/4"

NORMAL STRESS (KSI)

Fig. 25a   x = 0
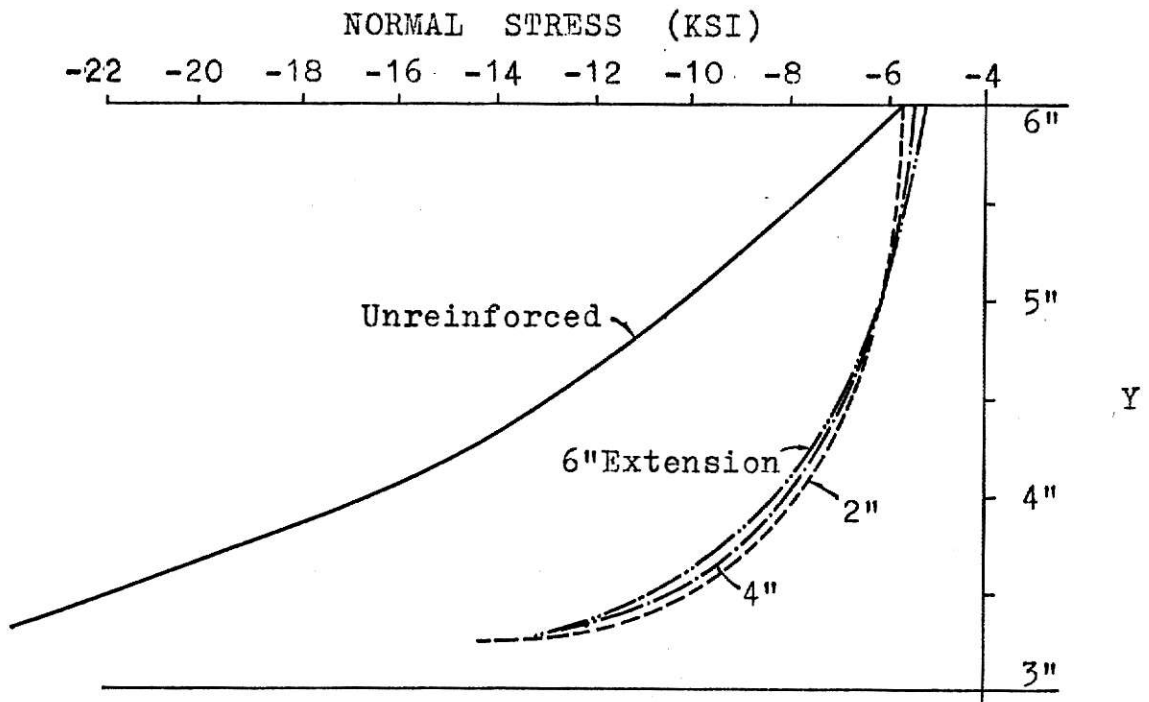
Fig. 25b   x = -4½"

Fig. 25   Effects of Reinforcement on Normal
Stresses for M/V = 40"

NORMAL STRESS (KSI)

-18 -16 -14 -12 -10 -8 -6 -4 -2 0

6"

5"

4"

Unreinforced

2"Extension

4"

3" Y

2"

1"

0

Fig. 25c $x = -4^3/4"$

NORMAL STRESS (KSI)

-18 -16 -14 -12 -10 -8 -6 -4 -2 0

6"

5"

2"Extension

4"

6"   4"

3" Y

2"

Unreinforced

1"

0

Fig. 25d $x = -7\frac{1}{2}"$

NORMAL STRESS (KSI)

-9 -8 -7 -6 -5 -4 -3 -2 -1 0

2"

6"

Unreinforced

4"Extension

Y

6"
5"
4"
3"
2"
1"
0

Fig. 25e   x = -10³/4"

NORMAL STRESS (KSI)

-9 -8 -7 -6 -5 -4 -3 -2 -1 0

2"Extension

Unreinforced

6"

4"

Y

6"

5"

4"

3"
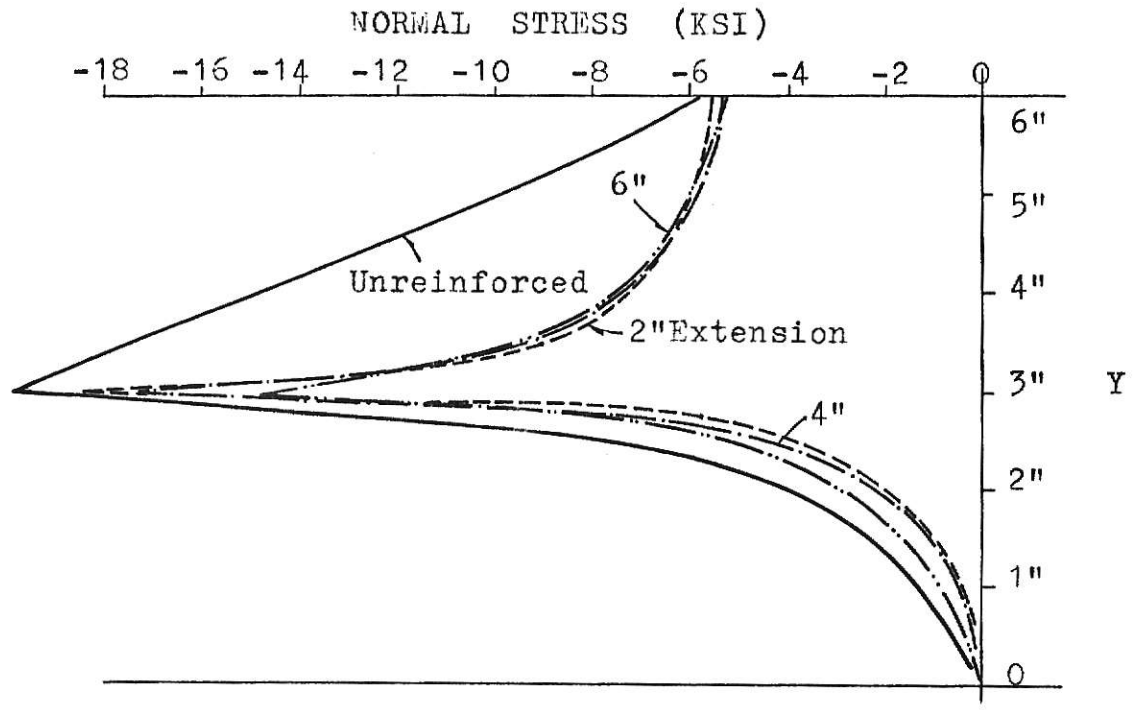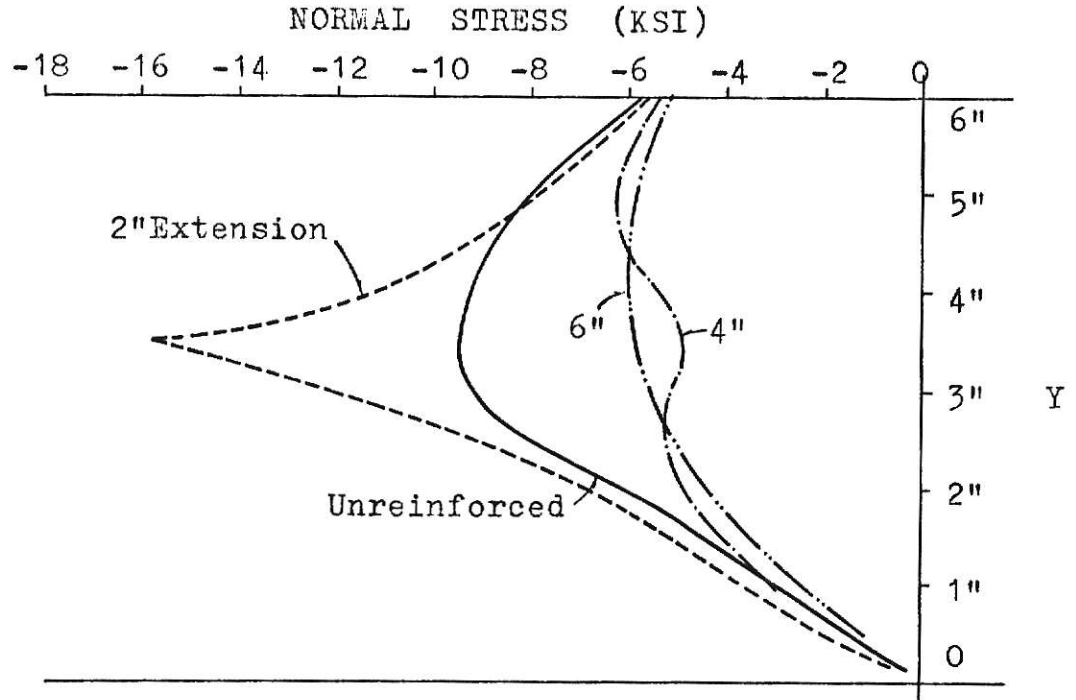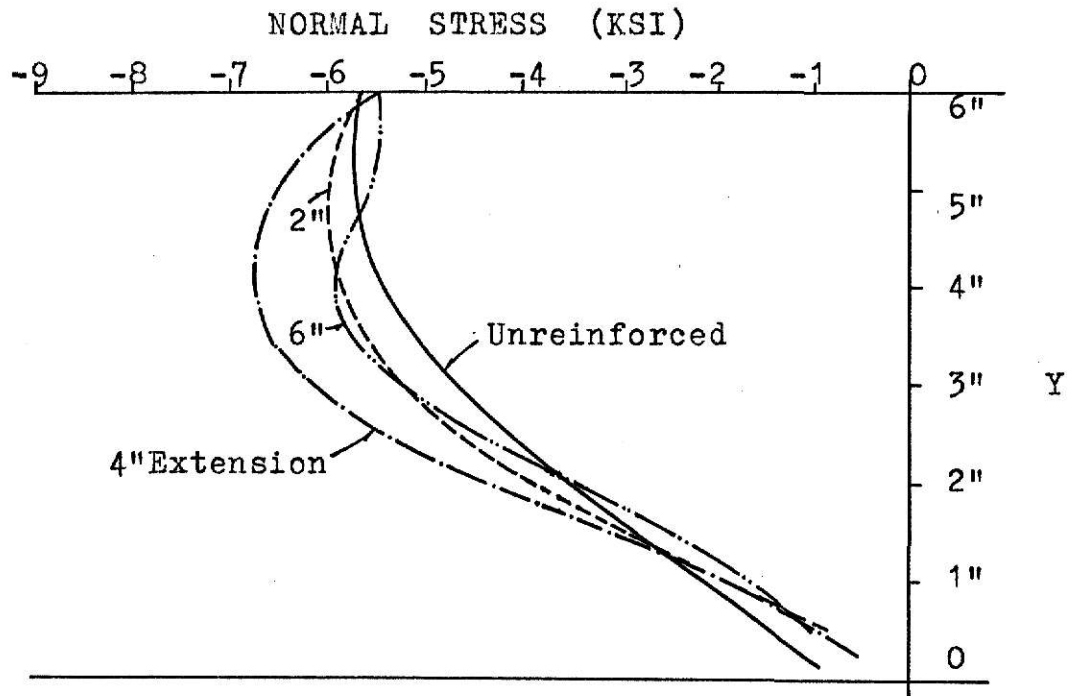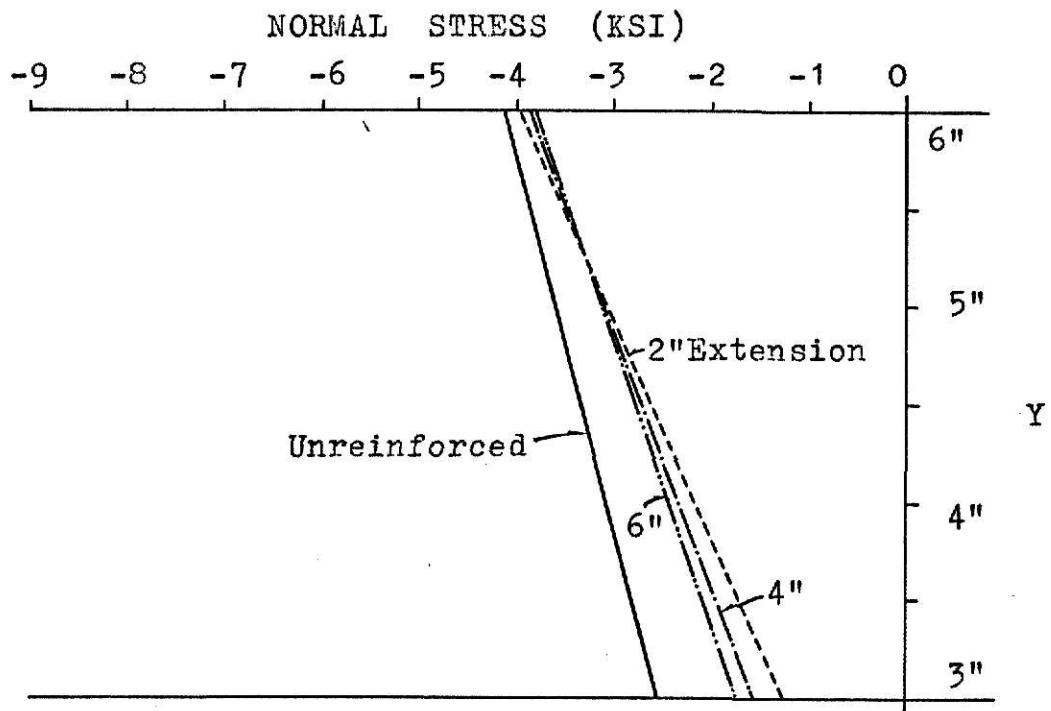
Fig. 26a   x = 0

Fig. 26   Effects of Reinforcement on Normal
          Stresses for M/V = 20"

NORMAL STRESS (KSI)

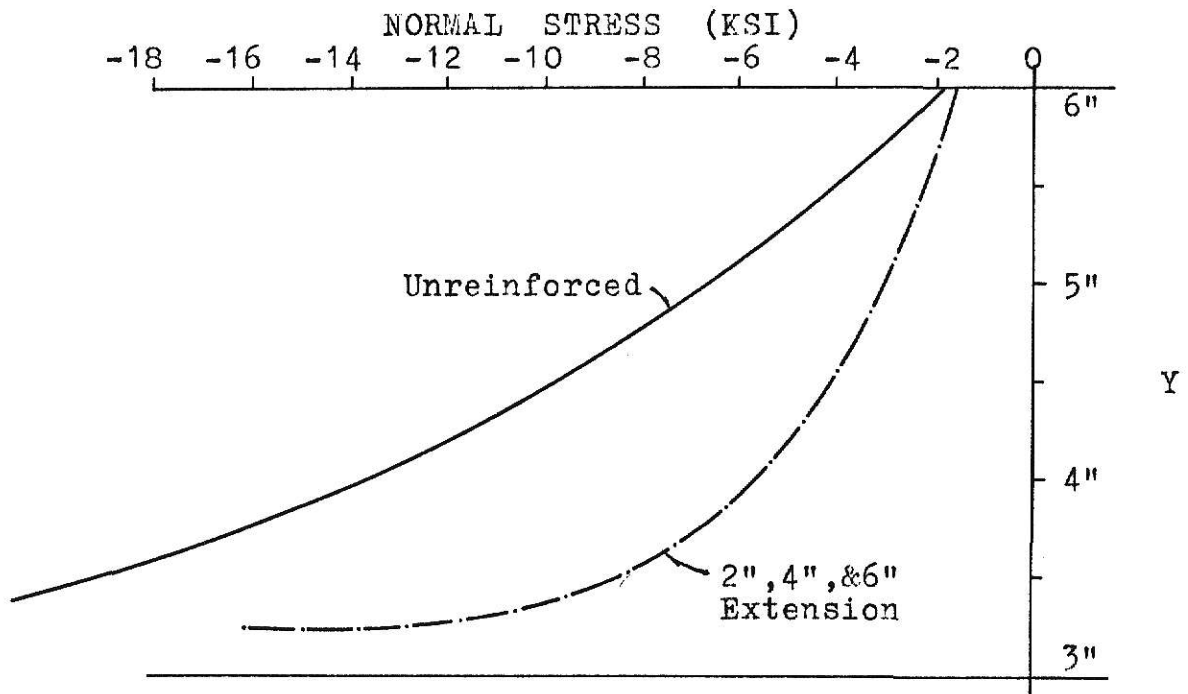-18   -16   -14   -12   -10   -8   -6   -4   -2   0

6"

5"

Unreinforced

Y

4"

2",4",&6"
Extension

3"

Fig. 26b   x = $-4\frac{1}{2}$"

NORMAL STRESS (KSI)

-18   -16   -14   -12   -10   -8   -6   -4   -2   0

6"

5"

4"   6"

4"

2"Extension

3"   Y

2"

Unreinforced

1"

0

Fig. 26c   x = $-4^3/4$"

NORMAL STRESS (KSI)

-18   -16   -14   -12   -10   -8   -6   -4   -2   0

Unreinforced

2"Extension

6"

4"

Y

6"
5"
4"
3"
2"
1"
0

Fig. 26d   x = -7½"

NORMAL STRESS (KSI)

-9   -8   -7   -6   -5   -4   -3   -2   -1   0

4"Extension

Unreinforced

6"

2"

Y

6"
5"
4"
3"
2"
1"
0
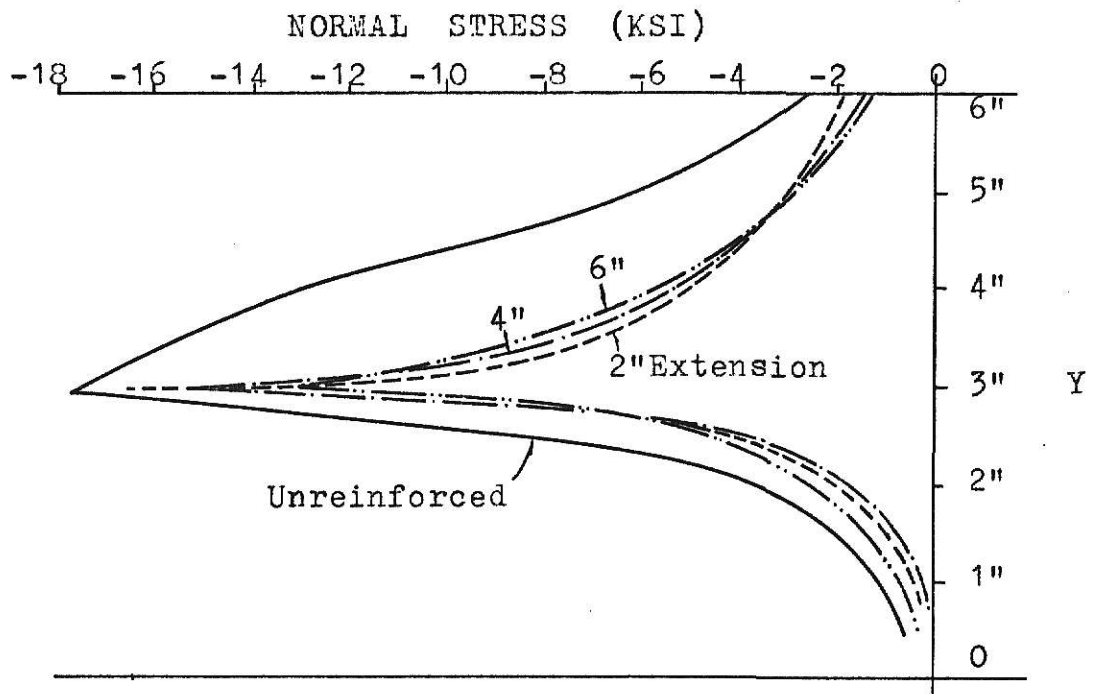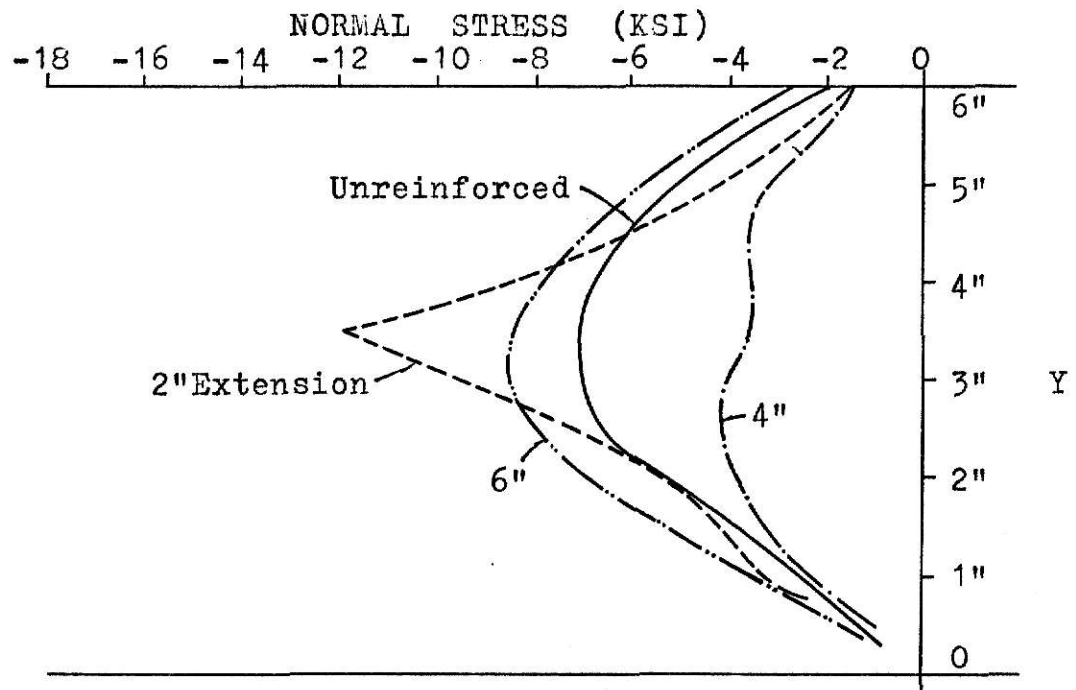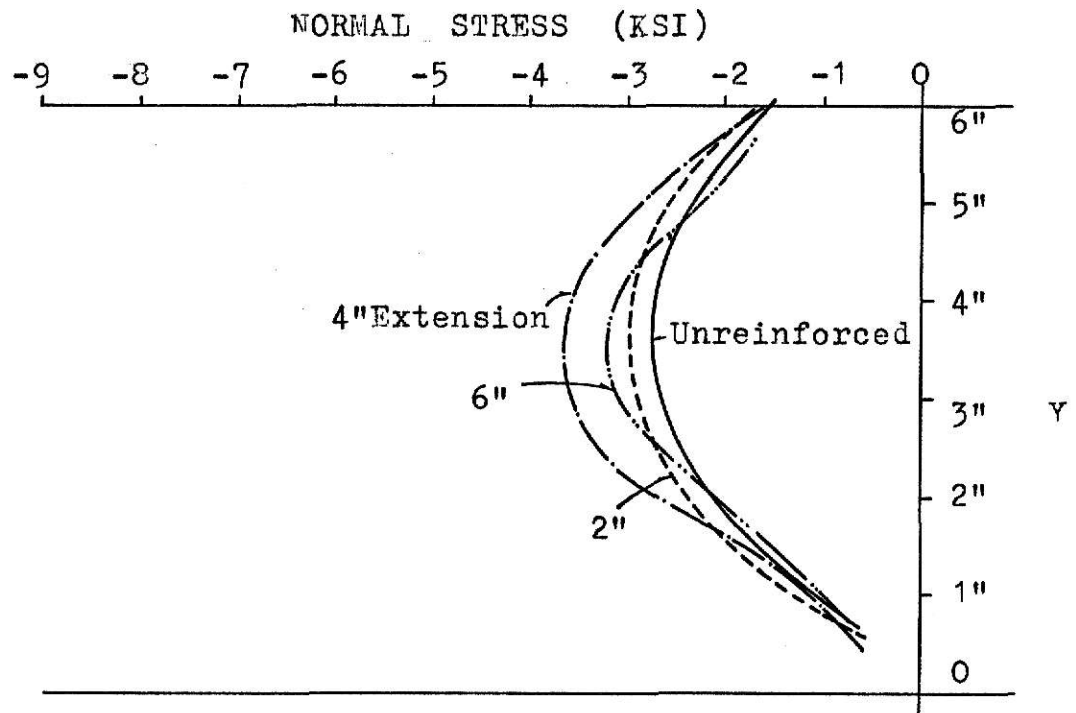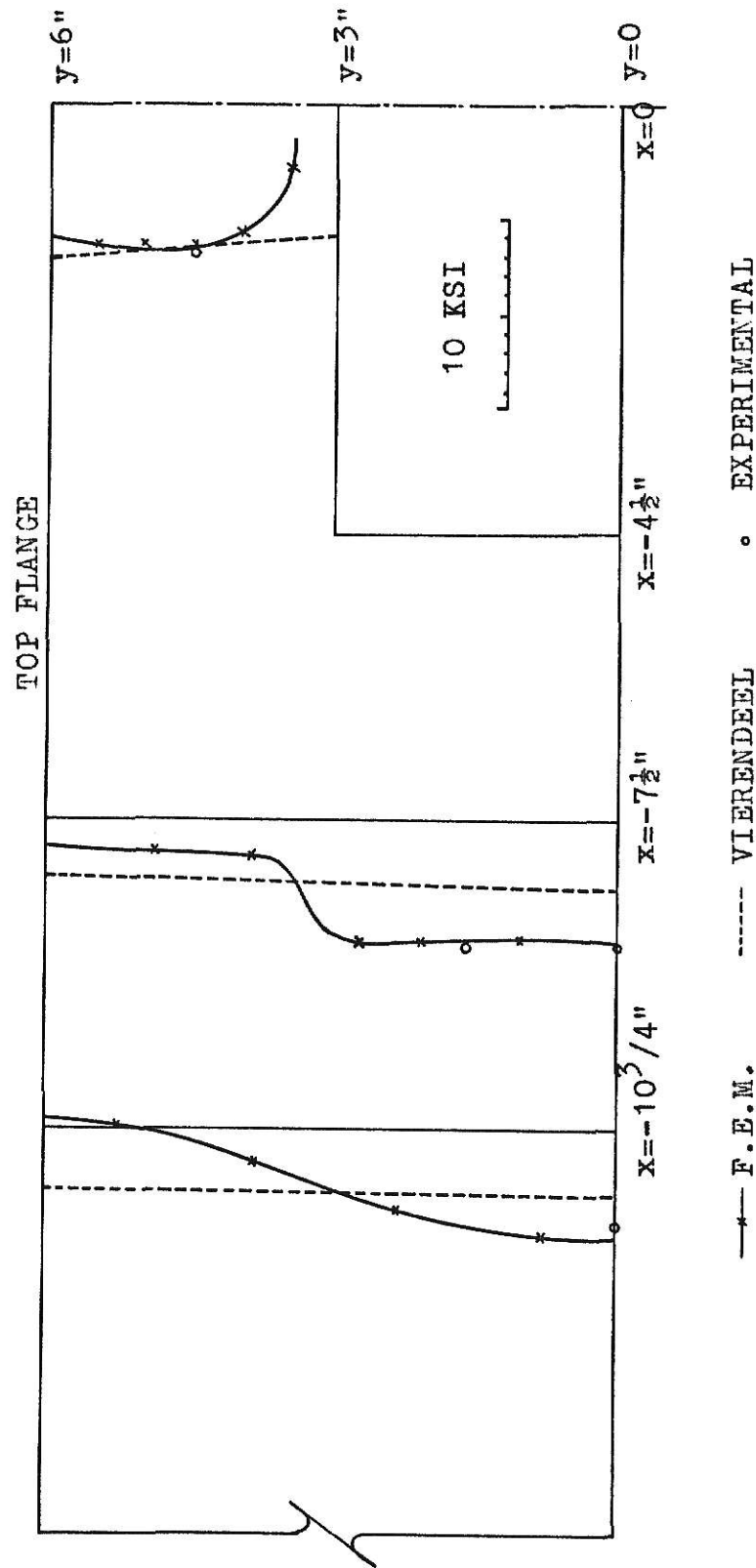
Fig. 26e   x = -10³/4"

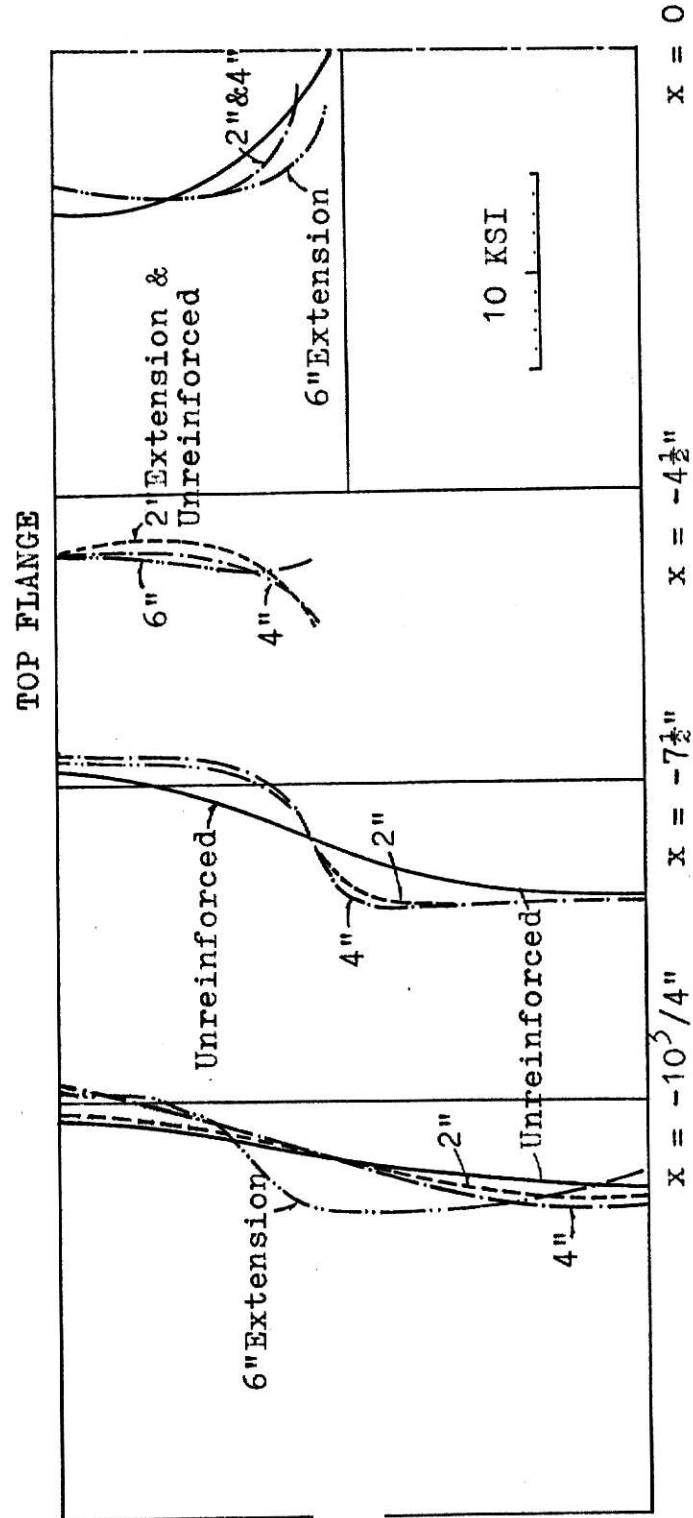Fig. 27 Shear Stresses From Different Approaches

Fig. 28 Effects of Reinforcement on Shear Stresses

VI. CONCLUSIONS

1. The predictions of normal stresses using the finite element analysis agree better with the experimental results than those obtained using the Vierendeel method. The normal stresses obtained at the top flange using the finite element method were in excellent agreement with the experimental results.

2. Even for the short 2" reinforcing extension, the advantage of reinforcing is very apparent. The stress distributions for different lengths of reinforcing do not change very much. However, one finds that the longer the reinforcing, the more the stresses were drawn from the flange to the reinforcing location.

3. The stress distribution patterns are generally the same. A sharp stress concentration is near the corner of opening, except in the region within 2" of the reinforcing termination.

4. Under the constant shear force, the maximum normal stress occurs at the top edge of the opening for low moment. It occurs at the flange for M-V ratios higher than 60". In other words, to relocate the opening may be one way to change the controlling stresses.

5. The shear stresses obtained using the finite element method were in excellent agreement with the experimental results for the 4" extension of reinforcing.

6. The effect of reinforcing on shear stresses is small except in the region near the reinforcing.

REFERENCES

1. Savin, G.N., "Stress Concentration Around Holes", International series of Monographs in Aeronautics and Astronautics, Pergamon Press, 1961.

2. Segner, E. P., Jr., "An Investigation of the Requirements for Reinforcement Around Large Rectangular Openings in the Webs of Wide-Flange Beams Subjected to Bending Moment and Shear", Texas Engineering Experiment Station, Project No. 30-422, Report No. E-81-62, College Station, Texas, 1963.

3. Cooper, P. B., and Snell, R. R., "Test on Beams with Reinforced Web Openings", Journal of the Structural Division, ASCE, Vol. 98, No. ST3, March, 1972.

4. Muskhelishvili, N. I., "Some Basic Problems of the Mathematical Theory of Elasticity", 2nd Edition, P. Noordhoff Ltd., Croningen, The Netherlands, 1963.

5. Joseph, J. A., and Brock, J. S., "The Stresses Around a Small Opening in a Beam Subjected to Pure Bending", Journal of Applied Mechanics, Vol. 17, No. 4, 1950.

6. Heller, S. R., Jr., Brock, J. S., and Bart, R., "The Stresses Around a Rectangular Opening with Rounded Corners in a Uniformly Loaded Plate", Proc., 3th National Congress of Applied Mechanics, 1958.

7. Heller, S. R. Jr., Brock, J. S., and Bart, R., "The Stress Around a Rectangular Opening with Rounded Corners in a Beam Subjected to Bending with Shear", Proc., 4th National Congress of Applied Mechanics, 1962.

8. Snell, R. R., "Reinforcing for a Rectangular Opening in a Plate", Journal of Structural Division, ASCE, Vol. 91, No. ST4, Aug., 1965.

9. Bower, J. E., "Elastic Stresses Around Web Holes in Wide Flange Beams", Journal of the Structural Division, ASCE, Vol. 92, No. ST2, April, 1966.

10. Bower, J. E., "Experimental Stresses in Wide Flange Beams with Holes", Journal of the Structural Division, ASCE, Vol. 92, No. ST5, Oct., 1966.

11. Redwood, R. G., and McCutheon, J. O., "Beam Tests with Unreinforced Web Openings", Journal of the Structural Division ASCE, Vol. 94, No. ST1, Jan., 1968.

12. Bower, J. E., "Design of Beams with Web Openings", Journal of the Structural Division ASCE, Vol. 94, No. ST, March, 1968.

13. Cheng, K., "Experimental Study of Beam with Web Opening", M.S. Thesis, Kansas State University, 1969.

14. Congdon, J. G., and Redwood, R. G., "Plastic Behavior of Beams with Reinforced Holes", Journal of the Structural Division, ASCE, Vol. 96, No. ST9, Sept., 1970.

15. Turner, M. J., Clough, R. W., Martin, H. C., and Topp, L. J., "Stiffness and Deflection Analysis of Comples Structures", Journal of Aeronautical Science, Vol. 23. No. 9, 1956.

16. Martin, H. C., "Introduction to Matrix Methods of Structural Analysis", McGraw-Hill Book Company, 1966.

17. Zienkiewicz, O. C., and Hollister, G. S., "Stress Analysis",
John Wiley & Son, 1965.

18. Zienkiewicz, O. C., and Cheng, Y. K., "The Finite Element Method
in Structural and Continuum Mechanics", McGraw-Hill Publishing Company
Ltd., Berkshire, England, 1967.

19. Timoshenko, S. P., "Theory of Plate and Shells", 2nd Edition, Mcgraw-
Hill Book Company, 1959.

20. Connor, J., and Will, G., "Computer-Aided Teaching of the Finite
Element Displacement Method", Research Report 69-23, Depart. of
Civil Eng., School of Eng., Massachusetts Institute of Technology.

21. Melosh, R. J., "Basis for Derivation of Matrices for the Direct
Stiffness Method", AIAA Journal, Vol. 1, No. 7, July 1963.

22. Grafton, P. E., and Strome, D. R., "Analysis of Axisymmetrical shells
by the Direct Stiffness Matrices", AIAA Journal, Vol. 1, No. 10,
Oct. 1963.

23. Pian, T. H. H., "Derivation of Element Stiffness Matrices", AIAA
Journal, Vol. 2, No. 3, March 1964.

24. Best, G. C., "A General Formula for Stiffness Matrices of Structural
Elements", AIAA Journal, Vol. 1, No. 8, Aug. 1963.

25. Mason, W. E., and Herrmann, L. R., "Elastic Analysis of Irregular
Shaped Prismatic Beams by the Method of Finite Elements", Technical
Report No. 67-1, Depart. of Civil Eng., Univ. of California, Davis.

26. Hsu, Y. I., "Plane Stress Finite Element Analysis of Beams with Web
Openings", Master's report, Depart. of Civil Engineering, Kansas
State University.

FINITE ELEMENT METHOD ANALYSIS

OF WIDE-FLANGE BEAM WITH REINFORCED OPENING

by

Farn-Shinn Liou

Diploma, Taipei Institute of Technology, 1964

————————

AN ABSTRACT OF MASTER'S REPORT

submitted in partial fulfillment of the

requirements for the degree

MASTER OF SCIENCE

Department of Civil Engineering

KANSAS STATE UNIVERSITY

Manhattan, Kansas

1972

ABSTRACT

Using the finite element analysis, this report presents a study of the effects of stress concentration in a wide-flange beam with a reinforced web opening. The direct stiffness method and the plane stress theory were reviewed. A 30" segment of the beam was divided into 275 elements to be studied. The ICES-STRUDL computer program was used to obtain the numerical results which were compared with the experimental results obtained at Kansas State University. The results were also compared with the results obtained using the Vierendeel method. For different lengths of reinforcing with the same cross section and location different results were obtained and compared. It was concluded that the finite element analysis provided good agreement with the experimental results. Also the stress concentrations near the corner of opening were decreased significantly when reinforcement was used.